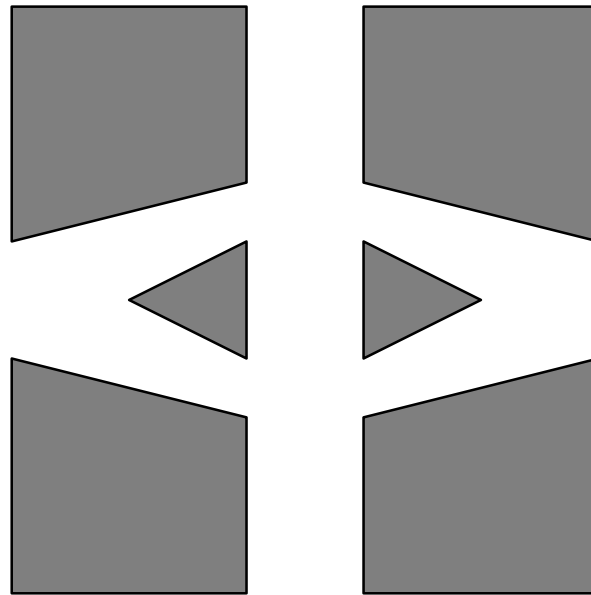


CHALMERS

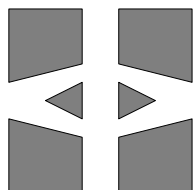
FINITE ELEMENT CENTER



PREPRINT 2003–11

Adaptive finite element/difference method for inverse elastic scattering waves

Larisa Beilina



Chalmers Finite Element Center
CHALMERS UNIVERSITY OF TECHNOLOGY
Göteborg Sweden 2003

CHALMERS FINITE ELEMENT CENTER

Preprint 2003–11

Adaptive finite element/difference method for inverse elastic scattering waves

Larisa Beilina



Chalmers Finite Element Center
Chalmers University of Technology
SE-412 96 Göteborg Sweden
Göteborg, July 2003

Adaptive finite element/difference method for inverse elastic scattering waves

Larisa Beilina

NO 2003–11

ISSN 1404–4382

Chalmers Finite Element Center
Chalmers University of Technology
SE–412 96 Göteborg
Sweden

Telephone: +46 (0)31 772 1000

Fax: +46 (0)31 772 3595

www.phi.chalmers.se

Printed in Sweden

Chalmers University of Technology
Göteborg, Sweden 2003

ADAPTIVE FINITE ELEMENT/DIFFERENCE METHOD FOR INVERSE ELASTIC SCATTERING WAVES

LARISA BEILINA

ABSTRACT. We apply an adaptive finite element/difference method for an inverse problem for time-dependent scattering of elastic waves in \mathbf{R}^d , $d = 2, 3$, where we seek to identify unknown material coefficients from measured wave-reflection data. Typical applications concern a large variety of inverse problems occurring in seismic prospectation, non-destructive testing and medical imaging.

We use an optimal control approach where we seek a density ρ and Lamé coefficients λ and μ which minimize the difference between computed and measured output data in a discrete L_2 norm. We solve the optimization problem by a quasi-Newton method, where in each step we compute the gradient by solving a forward and an adjoint elastic wave propagation problem.

For implementation of the inverse problem we use an adaptive hybrid finite element/difference method, where we combine the flexibility of finite elements and the efficiency of finite differences. We present computational results for three dimensional inverse scattering and use an adaptive mesh refinement algorithm based on an a posteriori error estimate, to improve the accuracy of the identification.

1. INTRODUCTION

This work is devoted to adaptive hybrid finite element/difference methods for an inverse scattering problem for a time-dependent elastic wave equation in the form of a parameter identification problem, where we seek to determine unknown material parameters with variation in space, from measured wave reflection data. Typical applications concern a large variety of inverse problems occurring in seismic prospectation, non-destructive testing and medical imaging.

The inverse problem is formulated as an optimal control problem, where we seek the material parameters for which the corresponding wave equation solution has a best least squares fit to measured data.

This constrained minimization problem is reformulated as the problem of finding a stationary point of a Lagrangian involving a forward elastic wave equation (the state equation), a backward elastic wave equation (the adjoint equation), and an equation expressing that the gradient with respect to the parameters vanishes. For efficient numerical solution of the forward and backward elastic wave equation we use the hybrid finite element/difference method developed in [10].

Date: 9th July 2003.

Larisa Beilina, Department of Mathematics, Chalmers University of Technology, S-412 96 Göteborg, Sweden, *email:* larisa@math.chalmers.se.

We prove an a posteriori error estimate for the error in the Lagrangian and present a corresponding adaptive algorithm for mesh adaption. We demonstrate in several numerical examples the performance of the inverse solver, involving the solution of the state equation, an adjoint state equation and computation of the gradient with respect to the parameters.

An outline of this paper is as follows: In Section 2 we present the mathematical model of the time-dependent wave equation in elastodynamics, in Section 3 we formulate the inverse scattering problem for the elastic wave equation, in Section 4 we present the finite element method, in Section 5 we present a fully discrete version, used in the computations. In Section 6 we prove a posteriori error estimate for the error in the Lagrangian, and in Section 8 we present computational results for reconstruction of the parameters in three dimensions.

2. THE WAVE EQUATION IN ELASTODYNAMICS

Wave propagation in a non-homogeneous anisotropic elastic medium occupying a bounded domain $\Omega \subset \mathbf{R}^d$, $d = 2, 3$, with boundary Γ , is described by the linear wave equation:

$$(2.1) \quad \begin{aligned} \rho \frac{\partial^2 v}{\partial t^2} - \nabla \cdot \tau &= f, & \text{in } \Omega \times (0, T), \\ \tau &= C \epsilon, & \text{in } \Omega \times (0, T), \\ v &= 0, \quad \frac{\partial v}{\partial t} = 0, & \text{in } \Omega, \end{aligned}$$

where $v(x, t) \in \mathbf{R}^d$, is the displacement, τ is the stress tensor, $\rho(x)$ is the density of the material depending on $x \in \Omega$, t is the time variable, T is a final time, and $f(x, t) \in \mathbf{R}^d$, is a given source function. Further, ϵ is the strain tensor with components

$$(2.2) \quad \epsilon_{ij} = \epsilon_{ij}(v) = \frac{1}{2} \left(\frac{\partial v_i}{\partial x_j} + \frac{\partial v_j}{\partial x_i} \right)$$

coupled to τ by Hooke's law

$$(2.3) \quad \tau_{ij} = \sum_{k=1}^d \sum_{l=1}^d C_{ijkl} \epsilon_{kl},$$

where C is a cyclic symmetric tensor, satisfying

$$(2.4) \quad C_{ijkl} = C_{klij} = C_{jkli}.$$

If the constants $C_{ijkl}(x)$ do not depend on x , then the material of the body is said to be homogeneous. If the constants $C_{ijkl}(x)$ do not depend on the choice of the coordinate system, then the material of the body is said to be isotropic at the point x .

In the isotropic case C can be written as

$$(2.5) \quad C_{ijkl} = \lambda \delta_{ij} \delta_{kl} + \mu (\delta_{ij} \delta_{kl} + \delta_{il} \delta_{jk}),$$

where δ_{ij} is Kronecker symbol, in which case (2.3) takes the form of Hooke's law:

$$(2.6) \quad \tau_{ij} = \lambda \delta_{ij} \sum_{k=1}^d \epsilon_{kk} + 2\mu \epsilon_{ij},$$

where λ and μ are the Lamé coefficients, depending on x , given by

$$(2.7) \quad \mu = \frac{E}{2(1+\nu)}, \quad \lambda = \frac{E\nu}{(1+\nu)(1-2\nu)},$$

where $E(x) > 0$ is the modulus of elasticity (Young modulus) and $0 < \nu < 1/2$ is the Poisson's ratio of the elastic material. Eliminating the strain tensor using Hooke's law we can verify the elastic wave equation in terms of v only. In the isotropic case with $d = 3$ (2.1) then takes the following form:

$$\begin{aligned} \rho \frac{\partial^2 v_1}{\partial t^2} &= \frac{\partial}{\partial x_1} \left((\lambda + 2\mu) \frac{\partial v_1}{\partial x_1} + \lambda \frac{\partial v_2}{\partial x_2} + \lambda \frac{\partial v_3}{\partial x_3} \right) \\ &\quad - \frac{\partial}{\partial x_2} \left(\mu \left(\frac{\partial v_1}{\partial x_2} + \frac{\partial v_2}{\partial x_1} \right) \right) \\ &\quad - \frac{\partial}{\partial x_3} \left(\mu \left(\frac{\partial v_1}{\partial x_3} + \frac{\partial v_3}{\partial x_1} \right) \right) = f_1, \\ \rho \frac{\partial^2 v_2}{\partial t^2} &= \frac{\partial}{\partial x_2} \left((\lambda + 2\mu) \frac{\partial v_2}{\partial x_2} + \lambda \frac{\partial v_1}{\partial x_1} + \lambda \frac{\partial v_3}{\partial x_3} \right) \\ &\quad - \frac{\partial}{\partial x_1} \left(\mu \left(\frac{\partial v_1}{\partial x_2} + \frac{\partial v_2}{\partial x_1} \right) \right) \\ &\quad - \frac{\partial}{\partial x_3} \left(\mu \left(\frac{\partial v_2}{\partial x_3} + \frac{\partial v_3}{\partial x_2} \right) \right) = f_2, \\ \rho \frac{\partial^2 v_3}{\partial t^2} &= \frac{\partial}{\partial x_3} \left((\lambda + 2\mu) \frac{\partial v_3}{\partial x_3} + \lambda \frac{\partial v_2}{\partial x_2} + \lambda \frac{\partial v_1}{\partial x_1} \right) \\ &\quad - \frac{\partial}{\partial x_2} \left(\mu \left(\frac{\partial v_2}{\partial x_3} + \frac{\partial v_3}{\partial x_2} \right) \right) \\ &\quad - \frac{\partial}{\partial x_1} \left(\mu \left(\frac{\partial v_1}{\partial x_3} + \frac{\partial v_3}{\partial x_1} \right) \right) = f_3, \end{aligned}$$

or in more compact vector form

$$(2.8) \quad \rho \frac{\partial^2 v}{\partial t^2} - \nabla \cdot (\mu \nabla v) - \nabla((\lambda + \mu) \nabla \cdot v) = f,$$

where $v = (v_1, v_2, v_3)$. Inserting a Helmholtz decomposition

$$v = \nabla \phi + \nabla \times \psi$$

with a scalar potential ϕ and a vector potential ψ into (2.8), we get

$$\rho \frac{\partial^2}{\partial t^2} (\nabla \phi + \nabla \times \psi) = \mu \Delta (\nabla \phi + \nabla \times \psi) + (\lambda + \mu) \nabla (\nabla \cdot (\nabla \phi + \nabla \times \psi)),$$

which using that

$$\begin{aligned}\nabla \cdot (\nabla \phi) &= \Delta \phi, \\ \nabla \cdot (\nabla \times \psi) &= 0,\end{aligned}$$

reduces to

$$\nabla \left(\rho \frac{\partial^2 \phi}{\partial t^2} - (\lambda + 2\mu) \Delta \phi \right) + \nabla \times \left(\rho \frac{\partial^2 \psi}{\partial t^2} - \mu \Delta \psi \right) = 0.$$

We conclude that if the potentials ϕ and ψ satisfy the wave equations

$$\begin{aligned}\rho \frac{\partial^2 \phi}{\partial t^2} - (\lambda + 2\mu) \Delta \phi &= 0, \\ \rho \frac{\partial^2 \psi}{\partial t^2} - \mu \Delta \psi &= 0,\end{aligned}$$

then $v = \nabla \phi + \nabla \times \psi$ satisfies (2.8). We note that $v = \nabla \phi$ corresponds to a pressure wave with speed

$$V_p = \left(\frac{\lambda + 2\mu}{\rho} \right)^{1/2},$$

and $v = \nabla \times \psi$ to a shear wave with speed

$$V_s = \left(\frac{\mu}{\rho} \right)^{1/2}.$$

In a pressure wave the displacement is parallel to the direction of wave propagation, and in a shear wave, it is orthogonal to the direction of propagation.

3. THE INVERSE SCATTERING PROBLEM

We consider the elastic wave equation in a non-homogeneous isotropic medium in a bounded domain $\Omega \subset \mathbf{R}^d$, $d = 2, 3$, with boundary Γ :

$$\begin{aligned}(3.1) \quad \rho \frac{\partial^2 v}{\partial t^2} - \mu \Delta v - (\lambda + \mu) \nabla (\nabla \cdot v) &= f \quad \text{in } \Omega \times (0, T), \\ v &= 0 \quad \text{on } \Gamma \times (0, T), \\ v(x, 0) = 0, \quad \frac{\partial v(x, 0)}{\partial t} &= 0 \quad \text{in } \Omega,\end{aligned}$$

with homogeneous boundary and initial data.

We formulate the inverse scattering problem for (3.1) as follows: Find the parameters $\rho(x)$, $\mu(x)$ and $\lambda(x)$, which minimize the quantity

$$\begin{aligned}(3.2) \quad E(v, \rho, \lambda, \mu) &= \frac{1}{2} \int_0^T \int_{\Omega} (v - \tilde{v})^2 \delta_{obs} \, dx dt \\ &+ \frac{1}{2} \gamma_1 \int_{\Omega} \rho^2 \, dx + \frac{1}{2} \gamma_2 \int_{\Omega} \mu^2 \, dx + \frac{1}{2} \gamma_3 \int_{\Omega} \lambda^2 \, dx,\end{aligned}$$

where \tilde{v} is observed time-data at a finite set of observation points x_{obs} , v satisfies (3.1) and thus depends on ρ , μ and λ , $\delta_{obs} = \sum \delta(x_{obs})$ is a sum of multiples of delta-functions $\delta(x_{obs})$ corresponding to the observation points, and γ_i , $i = 1, 2, 3$ are regularization parameters.

To approach this minimization problem, we introduce the Lagrangian

$$(3.3) \quad L(u) = E(v, \rho, \lambda, \mu) + \int_0^T \int_{\Omega} \left(-\rho \frac{\partial \alpha}{\partial t} \frac{\partial v}{\partial t} + \mu \nabla \alpha \nabla v + (\lambda + \mu) \nabla \cdot v \nabla \cdot \alpha - f \alpha \right) dx dt,$$

where $u = (v, \alpha, \rho, \mu, \lambda)$, and search for a stationary point u satisfying for all \bar{u}

$$(3.4) \quad L'(u; \bar{u}) = 0,$$

where $L'(u; \cdot)$ is the Jacobian of L , and we assume that $\alpha(\cdot, T) = \bar{\alpha}(\cdot, T) = 0$ and $v(\cdot, 0) = \bar{v}(\cdot, 0) = 0$.

The equation (3.4) expresses that for all u ,

$$(3.5) \quad 0 = L'_{\alpha}(u; \bar{\alpha}) = \int_0^T \int_{\Omega} \left(-\rho \frac{\partial \bar{\alpha}}{\partial t} \frac{\partial v}{\partial t} + \mu \nabla \bar{\alpha} \nabla v + (\lambda + \mu) \nabla \cdot v \nabla \cdot \bar{\alpha} - f \bar{\alpha} \right) dx dt,$$

$$(3.6) \quad 0 = L'_v(u; \bar{v}) = \int_0^T \int_{\Omega} (v - \bar{v}) \bar{v} \delta_{obs} dx dt + \int_0^T \int_{\Omega} -\rho \frac{\partial \alpha}{\partial t} \frac{\partial \bar{v}}{\partial t} + \mu \nabla \alpha \nabla \bar{v} + (\lambda + \mu) \nabla \cdot \bar{v} \nabla \cdot \alpha dx dt,$$

$$(3.7)$$

$$(3.8) \quad 0 = L'_{\rho}(u; \bar{\rho}) = - \int_0^T \int_{\Omega} \frac{\partial \alpha(x, t)}{\partial t} \frac{\partial v(x, t)}{\partial t} \bar{\rho} dx dt + \gamma_1 \int_{\Omega} \rho \bar{\rho} dx \quad x \in \Omega,$$

$$(3.9) \quad 0 = L'_{\mu}(u; \bar{\mu}) = \int_0^T \int_{\Omega} (\nabla \alpha \nabla v + \nabla \cdot v \nabla \cdot \alpha) \bar{\mu} dx dt + \gamma_2 \int_{\Omega} \mu \bar{\mu} dx \quad x \in \Omega,$$

$$(3.10) \quad 0 = L'_{\lambda}(u; \bar{\lambda}) = \int_0^T \int_{\Omega} \nabla \cdot v \nabla \cdot \alpha \bar{\lambda} dx dt + \gamma_3 \int_{\Omega} \lambda \bar{\lambda} dx \quad x \in \Omega.$$

The equation (3.5) is a weak form of the state equation (3.1), the equation (3.6) is a weak form of the adjoint state equation for the costate α :

$$(3.11) \quad \begin{aligned} \rho \frac{\partial^2 \alpha}{\partial t^2} - \mu \Delta \alpha - (\lambda + \mu) \nabla (\nabla \cdot \alpha) &= -(v - \bar{v}) \delta_{obs}, \quad x \in \Omega, \quad 0 < t < T, \\ \alpha(\cdot, T) &= \frac{\partial \alpha(\cdot, T)}{\partial t} = 0 \quad \text{in } \Omega, \\ \alpha &= 0 \quad \text{on } \Gamma \times (0, T), \end{aligned}$$

and (3.8) - (3.10) expresses stationarity with respect to (ρ, μ, λ) .

To solve the minimization problem we use a discrete form of the following steepest descent or gradient method starting from an initial guess $(\rho^0, \mu^0, \lambda^0)$ and computing a sequence $(\rho^n, \mu^n, \lambda^n)$ in the following steps:

- (1) Compute the solutions v^n of the forward problem (3.1) and compute the solution α^n of the adjoint problem (3.12) with $(\rho, \mu, \lambda) = (\rho^n, \mu^n, \lambda^n)$.
- (2) Update the (ρ, μ, λ) according to

$$\begin{aligned}
 (3.12) \quad \rho^{n+1}(x) &= \rho^n(x) - \beta_1^n \left(- \int_0^T \frac{\partial \alpha^n(x, t)}{\partial t} \frac{\partial v^n(x, t)}{\partial t} dt + \gamma_1 \rho^n(x) \right), \\
 \mu^{n+1}(x) &= \mu^n(x) - \beta_2^n \left(\int_0^T \nabla \alpha^n \nabla v^n + \nabla \cdot v^n \nabla \cdot \alpha^n + \gamma_2 \mu^n(x) \right), \\
 \lambda^{n+1}(x) &= \lambda^n(x) - \beta_3^n \left(\int_0^T \nabla \cdot v^n \nabla \cdot \alpha^n + \gamma_3 \lambda^n(x) \right),
 \end{aligned}$$

where the step lengths β_i^n are computed using the one-dimensional search algorithm given in [30]. More precisely, we use consider a quasi-Newton method with limited storage with the gradient method being a special case.

4. FINITE ELEMENT DISCRETIZATION

We now formulate a finite element method for the inverse problem (3.4) based on using continuous piecewise linear functions in space and time for the state and the costate, and piecewise constants in space for the parameters. We discretize $\Omega \times (0, T)$ in the usual way denoting by $K_h = \{K\}$ a partition of the domain Ω into elements K (triangles in \mathbf{R}^2 and tetrahedra in \mathbf{R}^3) with $h = h(x)$ being a mesh function representing the local diameter of the elements), and we let $J_\tau = \{J\}$ be a partition of the time interval $I = (0, T)$ into time intervals $J = (t_{k-1}, t_k]$ of uniform length $\tau = t_k - t_{k-1}$. In fully discrete form the resulting method corresponds to a centered finite difference approximation for the second order time derivative and a usual finite element approximation in space.

We introduce the finite element spaces V_h , W_h^v and W_h^α defined by :

$$(4.1) \quad V_h := \{v \in L_2(\Omega) : v \in P_0(K), \forall K \in K_h\},$$

$$(4.2) \quad W^v := \{w \in [H^1(\Omega \times I)]^3 : w(\cdot, 0) = 0, w|_\Gamma = 0\},$$

$$(4.3) \quad W^\alpha := \{w \in [H^1(\Omega \times I)]^3 : w(\cdot, T) = w|_\Gamma = 0\},$$

$$(4.4) \quad W_h^v := \{w \in W^v : w|_{K \times J} \in [P_1(K) \times P_1(J)]^3, \forall K \in K_h, \forall J \in J_\tau\},$$

$$(4.5) \quad W_h^\alpha := \{w \in W^\alpha : w|_{K \times J} \in [P_1(K) \times P_1(J)]^3, \forall K \in K_h, \forall J \in J_\tau\},$$

where $P_1(K)$ and $P_1(J)$ are the set of linear functions on K and J , respectively. We finally define $U_h = W_h^v \times W_h^\alpha \times V_h^3$. The finite element method for (3.4) can now be formulated as follows: Find $u_h \in U_h$ such that

$$(4.6) \quad L'(u_h; \bar{u}) = 0 \quad \forall \bar{u} \in U_h.$$

5. FULLY DISCRETE SCHEME

Expanding v, α in terms of the standard continuous piecewise linear functions $\varphi_i(x)$ in space and $\psi_i(t)$ in time and substituting this into (3.5 - 3.6), the following system of linear equations is obtained:

$$(5.1) \quad \begin{aligned} M(\mathbf{v}^{k+1} - 2\mathbf{v}^k + \mathbf{v}^{k-1}) &= \tau^2 F^k - \tau^2 K \left(\frac{1}{6} \mathbf{v}^{k-1} + \frac{2}{3} \mathbf{v}^k + \frac{1}{6} \mathbf{v}^{k+1} \right) \\ &- \tau^2 D \mathbf{v}^k, \end{aligned}$$

$$(5.2) \quad \begin{aligned} M(\boldsymbol{\alpha}^{k+1} - 2\boldsymbol{\alpha}^k + \boldsymbol{\alpha}^{k-1}) &= -\tau^2 S^k - \tau^2 K \left(\frac{1}{6} \boldsymbol{\alpha}^{k-1} + \frac{2}{3} \boldsymbol{\alpha}^k + \frac{1}{6} \boldsymbol{\alpha}^{k+1} \right) \\ &- \tau^2 D \boldsymbol{\alpha}^k, \end{aligned}$$

with initial conditions :

$$(5.3) \quad v(0) = 0, \quad \dot{v}(0) \approx 0,$$

$$(5.4) \quad \alpha(T) = 0, \quad \dot{\alpha}(T) \approx 0.$$

Here, M is the mass matrix in space, K is the stiffness matrix, D is the divergence matrix, $k = 1, 2, 3 \dots$ denotes the time level, F^k, S^k are the load vectors, \mathbf{v} is the nodal values of v , $\boldsymbol{\alpha}$ is the nodal values of α and τ is the time step.

The explicit formulas for the entries in system (5.1 - 5.2) at the element level can be given as:

$$(5.5) \quad M_{i,j}^e = (\rho \varphi_i, \varphi_j)_e,$$

$$(5.6) \quad K_{i,j}^e = (\mu \nabla \varphi_i, \nabla \varphi_j)_e,$$

$$(5.7) \quad D_{i,j}^e = ((\lambda + \mu) \nabla \cdot \varphi_i, \nabla \cdot \varphi_j)_e,$$

$$(5.8) \quad F_{j,m}^e = (f, \varphi_j \psi_m)_{e \times J},$$

$$(5.9) \quad S_{j,m}^e = (v - \tilde{v}, \varphi_j \psi_m)_{e \times J},$$

where $(\cdot, \cdot)_e$ denotes the $L_2(e)$ scalar product. The matrix M^e is the contribution from element e to the global assembled matrix in space M , K^e is the contribution from element e to the global assembled matrix K , D^e is the contribution from element e to the global assembled matrix D , F^e and S^e are the contributions from element e to the assembled source vectors F and in (3.1) and (3.12), respectively.

To obtain an explicit scheme we approximate M with the lumped mass matrix M^L , the diagonal approximation obtained by taking the row sum of M , see e.g. [18]. By multiplying (5.1) - (5.2) with $(M^L)^{-1}$ and replacing the terms $\frac{1}{6} \mathbf{v}^{k-1} + \frac{2}{3} \mathbf{v}^k + \frac{1}{6} \mathbf{v}^{k+1}$ and $\frac{1}{6} \boldsymbol{\alpha}^{k-1} + \frac{2}{3} \boldsymbol{\alpha}^k + \frac{1}{6} \boldsymbol{\alpha}^{k+1}$ by \mathbf{v}^k and $\boldsymbol{\alpha}^k$, respectively, we obtain an efficient explicit formulation:

$$(5.10) \quad \begin{aligned} \mathbf{v}^{k+1} &= \tau^2 (M^L)^{-1} F^k + 2\mathbf{v}^k - \tau^2 (M^L)^{-1} K \mathbf{v}^k \\ &- \tau^2 (M^L)^{-1} D \mathbf{v}^k - \mathbf{v}^{k-1}, \end{aligned}$$

$$(5.11) \quad \begin{aligned} \boldsymbol{\alpha}^{k+1} &= -\tau^2 (M^L)^{-1} S^k + 2\boldsymbol{\alpha}^k - \tau^2 (M^L)^{-1} K \boldsymbol{\alpha}^k \\ &- \tau^2 (M^L)^{-1} D \boldsymbol{\alpha}^k - \boldsymbol{\alpha}^{k+1}. \end{aligned}$$

The discrete version of the parameter gradient equations take the form:

$$(5.12) \quad \begin{aligned} 0 = L'_\rho(u; \bar{\rho}) &= - \int_0^T \int_\Omega \frac{\partial \alpha_h}{\partial t} \frac{\partial v_h}{\partial t} \bar{\rho} \, dx dt \\ &+ \gamma_1 \int_\Omega \rho_h \bar{\rho} \, dx, \forall \bar{\rho} \in V_h, \end{aligned}$$

$$(5.13) \quad \begin{aligned} 0 = L'_\mu(u; \bar{\mu}) &= \int_0^T \int_\Omega (\nabla \alpha_h \nabla v_h + \nabla \cdot v_h \nabla \cdot \alpha_h) \bar{\mu} \, dx dt \\ &+ \gamma_2 \int_\Omega \mu_h \bar{\mu} \, dx \, \forall \bar{\mu} \in V_h, \end{aligned}$$

$$(5.14) \quad \begin{aligned} 0 = L'_\lambda(u; \bar{\lambda}) &= \int_0^T \int_\Omega \nabla \cdot v_h \nabla \cdot \alpha_h \bar{\lambda} \, dx dt \\ &+ \gamma_3 \int_\Omega \lambda_h \bar{\lambda} \, dx, \, \forall \bar{\lambda} \in V_h. \end{aligned}$$

6. AN A POSTERIORI ERROR ESTIMATE FOR THE LAGRANGIAN AND AN ADAPTIVE ALGORITHM

We now prove an a posteriori error estimate for the Lagrangian. We start by writing an equation for the error e in the Lagrangian as

$$\begin{aligned} e = L(u) - L(u_h) &= \int_0^1 \frac{d}{d\epsilon} L(\epsilon u + (1 - \epsilon)u_h) d\epsilon \\ &= \int_0^1 L'(\epsilon u + (1 - \epsilon)u_h; u - u_h) d\epsilon \\ &= L'(u_h; u - u_h) + R, \end{aligned}$$

where R is a second order remainder term. Using the Galerkin orthogonality (4.6) and the splitting $u - u_h = (u - u_h^I) + (u_h^I - u_h)$, where u_h^I denotes an interpolant of $u \in U_h$, and neglecting the term R , we get:

$$(6.1) \quad e \approx L'(u_h)(u - u_h^I) = I_1 + I_2 + I_3 + I_4 + I_5,$$

where

$$(6.2) \quad I_1 = \int_0^T \int_{\Omega} -\rho_h \frac{\partial(\alpha - \alpha_h^I)}{\partial t} \frac{\partial v_h}{\partial t} + \mu_h \nabla(\alpha - \alpha_h^I) \nabla v_h \\ + (\lambda_h + \mu_h)(\nabla \cdot v_h \nabla \cdot (\alpha - \alpha_h^I)) - f(\alpha - \alpha_h^I) \, dx dt,$$

$$(6.3) \quad I_2 = \int_0^T \int_{\Omega} (v_h - \tilde{v})(v - v_h^I) \delta_{obs} \, dx dt \\ + \int_0^T \int_{\Omega} -\rho_h \frac{\partial \alpha_h}{\partial t} \frac{\partial(v - v_h^I)}{\partial t} + \mu_h \nabla \alpha_h \nabla(v - v_h^I) \\ + (\lambda_h + \mu_h) \nabla \cdot (v - v_h^I) \nabla \cdot \alpha_h \, dx dt,$$

$$(6.4) \quad I_3 = - \int_0^T \int_{\Omega} \frac{\partial \alpha_h(x, t)}{\partial t} \frac{\partial v_h(x, t)}{\partial t} (\rho - \rho_h^I) \, dx dt + \int_{\Omega} \rho_h (\rho - \rho_h^I) \, dx,$$

$$(6.5) \quad I_4 = \int_0^T \int_{\Omega} (\nabla \alpha_h \nabla v_h + \nabla \cdot v_h \nabla \cdot \alpha_h) (\mu - \mu_h^I) \, dx dt + \int_{\Omega} \mu_h (\mu - \mu_h^I) \, dx,$$

$$(6.6) \quad I_5 = \int_0^T \int_{\Omega} (\nabla \cdot v_h \nabla \cdot \alpha_h) (\lambda - \lambda_h^I) \, dx dt + \int_{\Omega} \lambda_h (\lambda - \lambda_h^I) \, dx.$$

To estimate (6.3) we integrate by parts in the first, second and third terms to get (neglecting terms with derivatives on the coefficients):

$$(6.7) \quad |I_1| = \left| \int_0^T \int_{\Omega} \rho_h \frac{\partial^2 v_h}{\partial t^2} (\alpha - \alpha_h^I) - \mu_h \Delta v_h (\alpha - \alpha_h^I) \right. \\ - (\lambda_h + \mu_h) \nabla(\nabla \cdot v_h)(\alpha - \alpha_h^I) - f(\alpha - \alpha_h^I) \, dx dt \\ + \sum_K \int_0^T \int_{\partial K} \mu_h \frac{\partial v_h}{\partial n_K} (\alpha - \alpha_h^I) \, ds dt \\ \left. - \sum_k \int_{\Omega} \rho_h \left[\frac{\partial v_h}{\partial t}(t_k) \right] (\alpha - \alpha_h^I)(t_k) \, dx \right|,$$

where $\frac{\partial v_h}{\partial n_K}$ results from the integration by parts in space and denotes the derivative of v_h in the outward normal direction n_K of the boundary ∂K of element K , and $\left[\frac{\partial v_h}{\partial t} \right]$, denoting the jump in time of $\frac{\partial v_h}{\partial t}$, results from integration by parts in time. In the second term of the (6.7) we sum over the element boundaries, and each internal side $S \in S_h$ occurs twice. Denoting by $\partial_s v_h$ the derivative of a function v_h in one of the normal directions of each side S , we can write

$$(6.8) \quad \sum_K \int_{\partial K} \mu_h \frac{\partial v_h}{\partial n_K} (\alpha - \alpha_h^I) \, ds = \sum_S \int_S \mu_h [\partial_s v_h] (\alpha - \alpha_h^I) \, ds,$$

where $[\partial_s v_h]$ is jump in the derivative ∂v_h computed from the two triangles sharing S . We distribute each jump equally to the two sharing triangles and return to a sum over

elements edges ∂K :

$$(6.9) \quad \sum_S \int_S \mu_h [\partial_s v_h] \cdot (\alpha - \alpha_h^I) \, ds = \sum_K \frac{1}{2} h_K^{-1} \int_{\partial K} \mu_h [\partial_s v_h] (\alpha - \alpha_h^I) h_K \, ds.$$

We formally set $dx = h_K ds$ and replace the integrals over the element boundaries ∂K by integrals over the elements K , to get:

$$(6.10) \quad \left| \sum_K \frac{1}{2} h_K^{-1} \int_{\partial K} \mu_h [\partial_s v_h] (\alpha - \alpha_h^I) h_K \, ds \right| \leq C \max_{S \subset \partial K} h_K^{-1} \int_{\Omega} \mu_h |[\partial_s v_h]| |(\alpha - \alpha_h^I)| \, dx,$$

where $[\partial_s v_h]|_K = \max_{S \subset \partial K} [\partial_s v_h]|_S$. Here and below by C we denote various positive constants of moderate size.

In a similar way we can estimate the third term in (6.7):

$$\begin{aligned} \left| \sum_k \int_{\Omega} \rho_h \left[\frac{\partial v_h}{\partial t}(t_k) \right] (\alpha - \alpha_h^I)(t_k) \, dx \right| &\leq \sum_k \int_{\Omega} \rho_h \tau^{-1} \cdot \left| \left[\frac{\partial v_h}{\partial t}(t_k) \right] \right| \cdot |(\alpha - \alpha_h^I)(t_k)| \, \tau dx \\ &\leq C \sum_k \int_{J_{\tau}} \int_{\Omega} \rho_h \tau^{-1} \cdot |[\partial v_{ht_k}]| \cdot |(\alpha - \alpha_h^I)| \, dx dt \\ &= C \int_0^T \int_{\Omega} \rho_h \tau^{-1} \cdot |[\partial v_{ht}]| \cdot |(\alpha - \alpha_h^I)| \, dx dt, \end{aligned}$$

where

$$(6.11) \quad [\partial v_{ht_k}] = \max_k \left(\left[\frac{\partial v_h}{\partial t}(t_k) \right], \left[\frac{\partial v_h}{\partial t}(t_{k+1}) \right] \right),$$

$$(6.12) \quad [\partial v_{ht}] = [\partial v_{ht_k}] \quad \text{on } J_{\tau}.$$

Substituting both above expressions for the second and third terms in (6.7), we get:

$$\begin{aligned}
|I_1| &\leq \int_0^T \int_{\Omega} \left| \rho_h \frac{\partial^2 v_h}{\partial t^2} - \mu_h \Delta v_h \right. \\
&\quad - (\mu_h + \lambda_h) \nabla(\nabla \cdot v_h) - f \left. \right| \cdot |(\alpha - \alpha_h^I)| \, dxdt \\
&\quad + \mu_h \int_0^T \int_{\Omega} \max_{S \subset \partial K} h_k^{-1} \cdot |[\partial_s v_h]| \cdot |(\alpha - \alpha_h^I)| \, dxdt \\
&\quad + \rho_h \int_0^T \int_{\Omega} \tau^{-1} \cdot |[\partial v_{ht}]| \cdot |(\alpha - \alpha_h^I)| \, dxdt \\
&\leq C \int_0^T \int_{\Omega} \left| \rho_h \frac{\partial^2 v_h}{\partial t^2} - \mu_h \Delta v_h \right. \\
&\quad - (\mu_h + \lambda_h) \nabla(\nabla \cdot v_h) - f \left. \right| \cdot \left(\tau^2 \left| \frac{\partial^2 \alpha}{\partial t^2} \right| + h^2 |D_x^2 \alpha| \right) \, dxdt \\
&\quad + C \mu_h \int_0^T \int_{\Omega} \max_{S \subset \partial K} h_k^{-1} \cdot |[\partial_s v_h]| \cdot \left(\tau^2 \left| \frac{\partial^2 \alpha}{\partial t^2} \right| + h^2 |D_x^2 \alpha| \right) \, dxdt \\
(6.13) \quad &\quad + C \rho_h \int_0^T \int_{\Omega} \tau^{-1} \cdot |[\partial v_{ht}]| \cdot \left(\tau^2 \left| \frac{\partial^2 \alpha}{\partial t^2} \right| + h^2 |D_x^2 \alpha| \right) \, dxdt,
\end{aligned}$$

where we used standard interpolation estimates for $\alpha - \alpha_h^I$, and C denotes interpolation constants. Next, the terms $\frac{\partial^2 v_h}{\partial t^2}$, Δv_h , $\nabla(\nabla \cdot v_h)$ disappear in the first integral in (6.13) (v_h is continuous piecewise linear function). We estimate $\frac{\partial^2 \alpha}{\partial t^2} \approx \frac{[\frac{\partial \alpha_h}{\partial t}]}{\tau}$ and $D_x^2 \alpha \approx \frac{[\frac{\partial \alpha_h}{\partial n}]}{h}$ to get:

$$\begin{aligned}
(6.14) \quad |I_1| &\leq C \int_0^T \int_{\Omega} |f| \cdot \left(\tau^2 \left| \frac{[\frac{\partial \alpha_h}{\partial t}]}{\tau} \right| + h^2 \left| \frac{[\frac{\partial \alpha_h}{\partial n}]}{h} \right| \right) \, dxdt \\
&\quad + C \mu_h \int_0^T \int_{\Omega} \max_{S \subset \partial K} h_k^{-1} |[\partial_s v_h]| \cdot \left(\tau^2 \left| \frac{[\frac{\partial \alpha_h}{\partial t}]}{\tau} \right| + h^2 \left| \frac{[\frac{\partial \alpha_h}{\partial n}]}{h} \right| \right) \, dxdt \\
&\quad + C \rho_h \int_0^T \int_{\Omega} \tau^{-1} |[\partial v_{ht}]| \cdot \left(\tau^2 \left| \frac{[\frac{\partial \alpha_h}{\partial t}]}{\tau} \right| + h^2 \left| \frac{[\frac{\partial \alpha_h}{\partial n}]}{h} \right| \right) \, dxdt.
\end{aligned}$$

We estimate I_2 similarly:

$$\begin{aligned}
|I_2| &\leq \int_0^T \int_{\Omega} \left| \rho_h \frac{\partial^2 \alpha_h}{\partial t^2} (v - v_h^I) - \mu_h \Delta \alpha_h (v - v_h^I) \right. \\
&\quad - (\lambda_h + \mu_h) \nabla (\nabla \cdot \alpha_h) (v - v_h^I) + (v_h - \tilde{v})(v - v_h^I) \left. \right| dx dt \\
&\quad + C \mu_h \int_0^T \int_{\Omega} \max_{S \subset \partial K} h_k^{-1} \cdot |[\partial_s \alpha_h]| \cdot |(v - v_h^I)| dx dt \\
&\quad + C \rho_h \int_0^T \int_{\Omega} \tau^{-1} \cdot |[\partial \alpha_{ht}]| \cdot |(v - v_h^I)| dx dt \\
&\leq C \int_0^T \int_{\Omega} \left| \rho_h \frac{\partial^2 \alpha_h}{\partial t^2} - \mu_h \Delta \alpha_h \right. \\
&\quad - (\lambda_h + \mu_h) \nabla (\nabla \cdot \alpha_h) + (v_h - \tilde{v}) \left. \right| \cdot |(v - v_h^I)| dx dt \\
&\quad + C \mu_h \int_0^T \int_{\Omega} \max_{S \subset \partial K} h_k^{-1} \cdot |[\partial_s \alpha_h]| \cdot |(v - v_h^I)| dx dt \\
&\quad + C \rho_h \int_0^T \int_{\Omega} \tau^{-1} \cdot |[\partial \alpha_{ht}]| \cdot |(v - v_h^I)| dx dt \\
&\leq C \int_0^T \int_{\Omega} \left| \left(\rho_h \frac{\partial^2 \alpha_h}{\partial t^2} - \mu_h \Delta \alpha_h - (\lambda_h + \mu_h) \nabla (\nabla \cdot \alpha_h) + (v_h - \tilde{v}) \right) \right| \cdot \\
&\quad \cdot \left(\tau^2 \left| \frac{\partial^2 v}{\partial t^2} \right| + h^2 |D_x^2 v| \right) dx dt \\
&\quad + C \mu_h \int_0^T \int_{\Omega} \max_{S \subset \partial K} h_k^{-1} \cdot |[\partial_s \alpha_h]| \cdot \left(\tau^2 \left| \frac{\partial^2 v}{\partial t^2} \right| + h^2 |D_x^2 v| \right) dx dt \\
&\quad + C \rho_h \int_0^T \int_{\Omega} \tau^{-1} \cdot |[\partial \alpha_{ht}]| \cdot \left(\tau^2 \left| \frac{\partial^2 v}{\partial t^2} \right| + h^2 |D_x^2 v| \right) dx dt \\
&\leq C \int_0^T \int_{\Omega} |(v_h - \tilde{v})| \cdot \left(\tau^2 \left| \frac{[\frac{\partial v_h}{\partial t}]}{\tau} \right| + h^2 \left| \frac{[\frac{\partial v_h}{\partial n}]}{h} \right| \right) dx dt \\
&\quad + C \mu_h \int_0^T \int_{\Omega} \max_{S \subset \partial K} h_k^{-1} |[\partial_s \alpha_h]| \cdot \left(\tau^2 \left| \frac{[\frac{\partial v_h}{\partial t}]}{\tau} \right| + h^2 \left| \frac{[\frac{\partial v_h}{\partial n}]}{h} \right| \right) dx dt \\
&\quad + C \rho_h \int_0^T \int_{\Omega} \tau^{-1} \cdot |[\partial \alpha_{ht}]| \cdot \left(\tau^2 \left| \frac{[\frac{\partial v_h}{\partial t}]}{\tau} \right| + h^2 \left| \frac{[\frac{\partial v_h}{\partial n}]}{h} \right| \right) dx dt.
\end{aligned}$$

To estimate I_3, I_4, I_5 we use a standard interpolation estimate of the form $\rho - \rho_h^I \approx hD_x\rho, \lambda - \lambda_h^I \approx hD_x\lambda, \mu - \mu_h^I \approx hD_x\mu$, to get:

$$\begin{aligned}
 (6.15) \quad |I_3| &\leq \int_0^T \int_{\Omega} \left| \frac{\partial \alpha_h(x, t)}{\partial t} \cdot \frac{\partial v_h(x, t)}{\partial t} \right| \cdot h \cdot |D_x \rho| \, dx dt \\
 &\quad + \int_{\Omega} |\rho_h| \cdot h \cdot |D_x \rho| \, dx \\
 &\leq C \int_0^T \int_{\Omega} \left| \frac{\partial \alpha_h(x, t)}{\partial t} \cdot \frac{\partial v_h(x, t)}{\partial t} \right| \cdot h \cdot \left| \frac{[\rho_h]}{h} \right| \, dx dt \\
 &\quad + C \int_{\Omega} |\rho_h| \cdot h \cdot \left| \frac{[\rho_h]}{h} \right| \, dx \\
 &\leq C \int_0^T \int_{\Omega} \left| \frac{\partial \alpha_h(x, t)}{\partial t} \cdot \frac{\partial v_h(x, t)}{\partial t} \right| \cdot |[\rho_h]| \, dx dt \\
 &\quad + C \int_{\Omega} |\rho_h| \cdot |[\rho_h]| \, dx.
 \end{aligned}$$

$$\begin{aligned}
 (6.16) \quad |I_4| &\leq \int_0^T \int_{\Omega} |\nabla \alpha_h \nabla v_h + (\nabla \cdot \alpha_h)(\nabla \cdot v_h)| \cdot h \cdot |D_x \mu| \, dx dt \\
 &\quad + \int_{\Omega} |\mu_h| \cdot h \cdot |D_x \mu| \, dx \\
 &\leq C \int_0^T \int_{\Omega} |\nabla \alpha_h \nabla v_h + \nabla \cdot \alpha_h \nabla \cdot v_h| \cdot h \cdot \left| \frac{[\mu_h]}{h} \right| \, dx dt \\
 &\quad + C \int_{\Omega} |\mu_h| \cdot h \cdot \left| \frac{[\mu_h]}{h} \right| \, dx \\
 &\leq C \int_0^T \int_{\Omega} |\nabla \alpha_h \nabla v_h + \nabla \cdot \alpha_h \nabla \cdot v_h| \cdot |[\mu_h]| \, dx dt \\
 &\quad + C \int_{\Omega} |\mu_h| \cdot |[\mu_h]| \, dx.
 \end{aligned}$$

$$\begin{aligned}
 (6.17) \quad |I_5| &\leq \int_0^T \int_{\Omega} |\nabla \cdot \alpha_h \nabla \cdot v_h| \cdot h \cdot |D_x \lambda| \, dx dt \\
 &\quad + \int_{\Omega} |\lambda_h| \cdot h \cdot |D_x \lambda| \, dx \\
 &\leq C \int_0^T \int_{\Omega} |\nabla \cdot \alpha_h \nabla \cdot v_h| \cdot h \cdot \left| \frac{[\lambda_h]}{h} \right| \, dx dt \\
 &\quad + C \int_{\Omega} |\lambda_h| \cdot h \cdot \left| \frac{[\lambda_h]}{h} \right| \, dx \\
 &\leq C \int_0^T \int_{\Omega} |\nabla \cdot \alpha_h \nabla \cdot v_h| \cdot |[\lambda_h]| \, dx dt \\
 &\quad + C \int_{\Omega} |\lambda_h| \cdot |[\lambda_h]| \, dx
 \end{aligned}$$

Defining the residuals

$$\begin{aligned}
R_{v_1} &= |f|, \quad R_{v_2} = \frac{\mu_h}{2} \max_{S \subset \partial K} h_k^{-1} |[\partial_s v_h]|, \quad R_{v_3} = \frac{\rho_h}{2} \tau^{-1} |[\partial v_{ht}]|, \\
R_{\alpha_1} &= |v_h - \tilde{v}|, \quad R_{\alpha_2} = \frac{\mu_h}{2} \max_{S \subset \partial K} h_k^{-1} |[\partial_s \alpha_h]|, \quad R_{\alpha_3} = \frac{\rho_h}{2} \tau^{-1} |[\partial \alpha_{ht}]|, \\
R_{\rho_1} &= \left| \frac{\partial \alpha_h}{\partial t} \frac{\partial v_h}{\partial t} \right|, \quad R_{\rho_2} = |\rho_h|, \\
R_{\mu_1} &= |\nabla \alpha_h \nabla v_h + \nabla \cdot \alpha_h \nabla \cdot v_h|, \quad R_{\mu_2} = |\mu_h|, \\
R_{\lambda_1} &= |\nabla \cdot \alpha_h \nabla \cdot v_h|, \quad R_{\lambda_2} = |\lambda_h|,
\end{aligned} \tag{6.18}$$

and interpolation errors in the form

$$\sigma_\alpha = C\tau \left| \left[\frac{\partial \alpha_h}{\partial t} \right] \right| + Ch \left| \left[\frac{\partial \alpha_h}{\partial n} \right] \right|, \tag{6.19}$$

$$\sigma_v = C\tau \left| \left[\frac{\partial v_h}{\partial t} \right] \right| + Ch \left| \left[\frac{\partial v_h}{\partial n} \right] \right|, \tag{6.20}$$

$$\sigma_\rho = C|[\rho_h]|, \quad \sigma_\mu = C|[\mu_h]|, \quad \sigma_\lambda = C|[\lambda_h]| \tag{6.21}$$

we obtain finally the following a posteriori estimate for the error in the Lagrangian

$$\begin{aligned}
(6.22) \quad |e| &\leq \int_0^T \int_\Omega R_{v_1} \sigma_\alpha \, dxdt + \int_0^T \int_\Omega R_{v_2} \sigma_\alpha \, dxdt + \int_0^T \int_\Omega R_{v_3} \sigma_\alpha \, dxdt \\
&+ \int_0^T \int_\Omega R_{\alpha_1} \sigma_v \, dxdt + \int_0^T \int_\Omega R_{\alpha_2} \sigma_v \, dxdt + \int_0^T \int_\Omega R_{\alpha_3} \sigma_v \, dxdt \\
&+ \int_0^T \int_\Omega R_{\rho_1} \sigma_\rho \, dxdt + \int_\Omega R_{\rho_2} \sigma_\rho \, dx + \int_0^T \int_\Omega R_{\mu_1} \sigma_\mu \, dxdt \\
&+ \int_\Omega R_{\mu_2} \sigma_\mu \, dx + \int_0^T \int_\Omega R_{\lambda_1} \sigma_\lambda \, dxdt + \int_\Omega R_{\lambda_2} \sigma_\lambda \, dx.
\end{aligned}$$

In the computations below we use the following variant of the gradient method with adaptive mesh selection:

1. Choose an initial mesh K_h and an initial time partition J_τ of the time interval $(0, T)$.
2. Compute the solution v^n on K_h and J_τ of the forward problem (3.1) with $(\rho, \mu, \lambda) = (\rho^n, \mu^n, \lambda^n)$.
3. Compute the solution α^n of the adjoint problem (3.12) on K_h and J_τ .

4. Update the (ρ, μ, λ) according to

$$(6.23) \quad \rho^{n+1}(x) = \rho^n(x) - \beta_1^n \left(- \int_0^T \frac{\partial \alpha^n(x, t)}{\partial t} \frac{\partial v^n(x, t)}{\partial t} dt + \gamma_1 \rho^n(x) \right),$$

$$(6.24) \quad \mu^{n+1}(x) = \mu^n(x) - \beta_2^n \left(\int_0^T \nabla \alpha^n \nabla v^n + \nabla \cdot v^n \nabla \cdot \alpha^n + \gamma_2 \mu^n(x) \right),$$

$$(6.25) \quad \lambda^{n+1}(x) = \lambda^n(x) - \beta_3^n \left(\int_0^T \nabla \cdot v^n \nabla \cdot \alpha^n + \gamma_3 \lambda^n(x) \right).$$

Make the steps 1 – 4 as long the gradient quickly decreases.

5. Refine all elements, where $(R_{\rho_1} + R_{\rho_2})\sigma_\rho + (R_{\mu_1} + R_{\mu_2})\sigma_\mu + (R_{\lambda_1} + R_{\lambda_2})\sigma_\lambda > tol$ and construct a new mesh K_h and a new time partition J_τ . Here tol is a tolerance chosen by the user. Return to 1.

7. AN A PRIORI ERROR ESTIMATE FOR THE ELASTIC WAVE EQUATION

In this section we prove an a priori error estimate for the following finite element method for (2.8) with $\lambda = \mu = \rho = 1$: Find $v_h^n \in V_{h,1}$, for $n = 1, \dots, N$ such that for $n = 1, \dots, N$,

$$(7.1) \quad (\partial_t^2 v_h^n, u) + (\nabla v_h^n, \nabla u) + (\nabla \cdot v_h^n, \nabla \cdot u) = (f^n, u) \quad \forall u \in V_{h,1},$$

where

$$(7.2) \quad \partial_t^2 v_h^n = \frac{v_h^{n+1} - 2v_h^n + v_h^{n-1}}{\tau^2},$$

and $v_h^0 = 0, v_h^1 = 0$, and

$$V_{h,1} := \{v \in H_0^1 : v \in [P_1(K)]^3, \forall K \in K_h\}.$$

For simplicity we assume here that h is constant.

For $w \in [H_0^1(\Omega)]^3$ we define the elliptic projection $\pi w \in V_{h,1}$ by

$$(7.3) \quad (\nabla \pi w, \nabla v) + (\nabla \cdot \pi w, \nabla \cdot v) = (\nabla w, \nabla v) + (\nabla \cdot w, \nabla \cdot v) \quad \forall v \in V_{h,1}.$$

We shall now estimate the difference between the discrete solution $v_h^n \in V_{h,1}$ and the elliptic projection $\pi v^n \in V_{h,1}$, and we define Θ^n

$$(7.4) \quad \Theta^n = v_h^n - \pi v^n.$$

Using the definition (7.3) and (2.8)), we obtain:

$$(7.5) \quad \begin{aligned} (\partial_t^2(\pi v^n), u) + (\nabla(\pi v^n), \nabla u) &+ (\nabla \cdot \pi v^n, \nabla \cdot u) \\ &= (\partial_t^2(\pi v^n), u) + (\nabla v^n, \nabla u) + (\nabla \cdot v^n, \nabla \cdot u) \\ &= (\rho^n, u) + (f^n, u) \quad \forall u \in V_{h,1}, \end{aligned}$$

where $\rho^n = \partial_t^2(\pi v^n) - \frac{\partial^2 v}{\partial t^2}(t_n)$ and $v^n = v(\cdot, t_n)$.

Subtracting (7.5) from (7.1) and using (7.4), we get the following error equation:

$$(7.6) \quad (\partial_t^2 \Theta^n, u) + (\nabla \Theta^n, \nabla u) + (\nabla \cdot \Theta^n, \nabla \cdot u) = -(\rho^n, u) \quad \forall u \in V_{h,1},$$

where

$$(7.7) \quad \|\rho^n\| \leq C(\tau^2\|(D_t^4 v)^n\| + h^2\|(D_x^2 D_t^2 v)^n\|).$$

We now choose

$$(7.8) \quad u = \frac{1}{2} \left(\frac{\Theta^{n+1} - \Theta^n}{\tau} + \frac{\Theta^n - \Theta^{n-1}}{\tau} \right) = \frac{1}{2\tau} (\Theta^{n+1} - \Theta^{n-1}),$$

and use the fact that

$$\partial_t^2 \Theta^n = \frac{\Theta^{n+1} - 2\Theta^n + \Theta^{n-1}}{\tau^2} = \frac{1}{\tau} \left(\frac{\Theta^{n+1} - \Theta^n}{\tau} - \frac{\Theta^n - \Theta^{n-1}}{\tau} \right),$$

to get

$$\begin{aligned} & \frac{1}{2\tau} \left(\frac{\Theta^{n+1} - \Theta^n}{\tau} - \frac{\Theta^n - \Theta^{n-1}}{\tau}, \frac{\Theta^{n+1} - \Theta^n}{\tau} + \frac{\Theta^n - \Theta^{n-1}}{\tau} \right) \\ & + \frac{1}{2\tau} (\nabla \Theta^n, \nabla (\Theta^{n+1} - \Theta^{n-1})) \\ & + \frac{1}{2\tau} (\nabla \cdot \Theta^n, \nabla \cdot (\Theta^{n+1} - \Theta^{n-1})) \\ & = \frac{1}{2\tau} (\rho^n, \Theta^{n+1} - \Theta^{n-1}), \end{aligned}$$

which reduces to

$$\begin{aligned} & \left(\frac{\|\Theta^{n+1} - \Theta^n\|^2}{\tau^2} - \frac{\|\Theta^n - \Theta^{n-1}\|^2}{\tau^2} \right) + (\nabla \Theta^n, \nabla (\Theta^{n+1} - \Theta^{n-1})) \\ & + (\nabla \cdot \Theta^n, \nabla \cdot (\Theta^{n+1} - \Theta^{n-1})) \\ (7.9) \quad & = (\rho^n, \Theta^{n+1} - \Theta^{n-1}). \end{aligned}$$

Summing over n in the first term of (7.9), we get assuming $\Theta^1 = \Theta^0 = 0$,

$$(7.10) \quad \sum_{n=1}^{N-1} \left(\frac{\|\Theta^{n+1} - \Theta^n\|^2}{\tau^2} - \frac{\|\Theta^n - \Theta^{n-1}\|^2}{\tau^2} \right) = \frac{\|\Theta^N - \Theta^{N-1}\|^2}{\tau^2},$$

and in the second and third terms of (7.9) :

$$\begin{aligned} & \sum_{n=1}^{N-1} (\nabla \Theta^n, \nabla (\Theta^{n+1} - \Theta^{n-1})) = (\nabla \Theta^N, \nabla \Theta^{N-1}), \\ (7.11) \quad & \sum_{n=1}^{N-1} (\nabla \cdot \Theta^n, \nabla \cdot (\Theta^{n+1} - \Theta^{n-1})) = (\nabla \cdot \Theta^N, \nabla \cdot \Theta^{N-1}), \end{aligned}$$

and thus we have:

$$\begin{aligned} & \frac{\|\Theta^N - \Theta^{N-1}\|^2}{\tau^2} + (\nabla \Theta^N, \nabla \Theta^{N-1}) \\ (7.12) \quad & + (\nabla \cdot \Theta^N, \nabla \cdot \Theta^{N-1}) = \sum_{n=1}^{N-1} (\rho^n, \Theta^{n+1} - \Theta^{n-1}). \end{aligned}$$

Using an inverse estimate with a constant c and assuming $\frac{c\tau}{h} \leq 1$, we have

$$\begin{aligned}
(\nabla \Theta^N, \nabla \Theta^{N-1}) &= (\nabla \Theta^N, \nabla \Theta^N) - (\nabla(\Theta^N - \Theta^{N-1}), \nabla \Theta^N) \\
&\geq \|\nabla \Theta^N\|^2 - \tau \left\| \frac{\nabla(\Theta^N - \Theta^{N-1})}{\tau} \right\| \cdot \|\nabla \Theta^N\| \\
&\geq \|\nabla \Theta^N\|^2 - \frac{c\tau}{h} \left\| \frac{(\Theta^N - \Theta^{N-1})}{\tau} \right\| \cdot \|\nabla \Theta^N\| \\
&\geq \frac{1}{2} \|\nabla \Theta^N\|^2 - \frac{1}{2} \left\| \frac{(\Theta^N - \Theta^{N-1})}{\tau} \right\|^2. \\
(\nabla \cdot \Theta^N, \nabla \cdot \Theta^{N-1}) &= (\nabla \cdot \Theta^N, \nabla \cdot \Theta^N) - (\nabla \cdot (\Theta^N - \Theta^{N-1}), \nabla \cdot \Theta^N) \\
&\geq \|\nabla \cdot \Theta^N\|^2 - \tau \left\| \frac{\nabla \cdot (\Theta^N - \Theta^{N-1})}{\tau} \right\| \cdot \|\nabla \cdot \Theta^N\| \\
&\geq \|\nabla \cdot \Theta^N\|^2 - \frac{c\tau}{h} \left\| \frac{(\Theta^N - \Theta^{N-1})}{\tau} \right\| \cdot \|\nabla \cdot \Theta^N\| \\
&\geq \frac{1}{2} \|\nabla \cdot \Theta^N\|^2 - \frac{1}{2} \left\| \frac{(\Theta^N - \Theta^{N-1})}{\tau} \right\|^2.
\end{aligned}$$

We conclude that

$$\begin{aligned}
(7.13) \quad & \frac{\|\Theta^N - \Theta^{N-1}\|^2}{\tau^2} + \|\nabla \Theta^N\|^2 + \|\nabla \cdot \Theta^N\|^2 \\
& \leq 2\tau \sum_{n=1}^{N-1} \left(\rho^n, \frac{\Theta^{n+1} - \Theta^{n-1}}{2\tau} \right).
\end{aligned}$$

Using the definition of ρ and (7.7), we get:

$$(7.14) \quad \sum_{n=1}^{N-1} \left(\rho^n, \frac{\Theta^{n+1} - \Theta^{n-1}}{2\tau} \right) \approx \sum_{n=1}^{N-1} (\tau^2 \|(D_t^4 v)^n\| + h^2 \|(D_x^2 D_t^2 v)^n\|) \partial_t \Theta.$$

We substitute this expression into (7.13) to get:

$$\begin{aligned}
\|\partial_t \Theta\|^2 + \|\nabla \Theta^N\|^2 + \|\nabla \cdot \Theta^N\|^2 \\
\leq 2\tau \left(\tau^2 \int_0^T \|(D_t^4 v)^n\| dt + h^2 \int_0^T \|(D_x^2 D_t^2 v)^n\| dt \right) \cdot \max_n \|\partial_t \Theta^n\|,
\end{aligned}$$

which gives the following a priori estimate for Θ :

$$(7.15) \quad \max_n \left(\left\| \frac{\partial \Theta^n}{\partial t} \right\| + \|\nabla \Theta^n\|^2 + \|\nabla \cdot \Theta^n\|^2 \right) \leq C(\tau^2 + h^2).$$

Using the fact that

$$(7.16) \quad \max_n (\|\partial_t(v - \pi v)^n\| + \|\nabla(v - \pi v)^n\| + \|\nabla \cdot (v - \pi v)^n\|) \leq C_1(\tau + h),$$

we get finally the following error estimate

$$(7.17) \quad \max_n (\|\partial_t(v - v_h)^n\| + \|\nabla(v - v_h)^n\| + \|\nabla \cdot (v - v_h)^n\|) \leq C_1(\tau + h).$$

No. of nodes	No. of elements	Forward problem		Adjoint problem	
		relat.time	time, sec	relat.time	time, sec
2783	13200	5.5530e-05	77.27	1.2392e-04	172.43
3603	17198	5.6375e-05	101.56	1.2524e-04	225.62
6898	36890	5.8518e-05	201.83	1.3064e-04	450.58

TABLE 1. Performance in the relative time (at the left column) and in the total time (at the right column) for the Forward and the Adjoint problems for Example 1.

8. NUMERICAL EXAMPLES

In this section we present computational results for our adaptive method for inverse elastic scattering in three dimensions with identification of the parameters ρ , λ and μ in (3.1). The computational domain is $\Omega = [0, 5.0] \times [0, 2.5] \times [0, 2.5]$, which is split into a finite element domain $\Omega_{FEM} = [0.3, 4.7] \times [0.3, 2.3] \times [0.3, 2.3]$ with a nonstructured mesh, and a surrounding domain Ω_{FDM} with a structured mesh. The space mesh in Ω_{FEM} consists of tetrahedra and in Ω_{FDM} of hexahedra with mesh size $h = 0.2$. We apply the hybrid finite element/difference method presented in [8] with finite elements in Ω_{FEM} and finite differences in Ω_{FDM} with absorbing boundary conditions on the boundary of Ω .

We present some examples with spherical pulses, generated at different points in Ω_{FDM} , which are given by the source function

$$(8.1) \quad f_1(x, x_0) = \begin{cases} 10^3 \sin^2 \pi t & \text{if } 0 \leq t \leq 0.1 \text{ and } |x - x_0| < r, \\ 0 & \text{otherwise;} \end{cases}$$

In all the computational tests we chose a time step to respect the CFL criterion:

$$(8.2) \quad \tau \leq h \sqrt{\frac{\rho}{\lambda + 3\mu}}.$$

First, we present examples of reconstructing the density ρ and the Lamé coefficients λ, μ , without adding noise to exact solution at the observation points. Then we present computational tests with adding 10% and 20% noise to solution at the observation points.

In all the examples we apply the quasi-Newton method and adaptive mesh refinement algorithm described in [9].

8.1. Example 1. In the first example we reconstruct the parameters ρ, λ and μ for the geometry presented in Fig. 1. We perform experiments with 4 spherical pulses, initialized in Ω_{FDM} . In Fig. 4 we present the computed exact solution on the coarse mesh of the problem (3.1) in Ω_{FDM} and the corresponding solution in Ω_{FEM} , using absorbing boundary conditions on the outer boundaries of Ω_{FDM} .

Appropriate initial values of the parameters in our experiments in the one dimensional optimization algorithm are $\alpha = 1.0$ and $\beta = 1.0$. We place the observation points at the surface of the Ω_{FDM} such that the observation points are located at the opposite side to the initialized pulses. We use a total of 22 observation points for this experiment.

m	2783 nodes	5426 nodes	7062 nodes	10951
1	0.00757337	0.00741713	0.00759996	0.00788409
	0.00635677	0.00648679	0.00631633	0.00656045
	0.00225678	0.00236001	0.00148713	0.00186424
	0.00237844	0.00234848	0.00762883	0.0016515
		0.00204324		0.0014904
		0.00178178		0.0013101
3				0.00122315
	0.00757337	0.00741713	0.00759996	0.00788409
	0.00697671	0.00699295	0.00724637	0.00749204
	0.00181184	0.00197857	0.00199707	0.00144807
	0.00168949	0.00186646		0.00120483
		0.00221419		
5	0.00757337	0.00741713	0.00759996	0.00788409
	0.00697671	0.00699295	0.00724637	0.00749204
	0.00181184	0.00197857	0.00199707	0.00144807
	0.00179391	0.00203611	0.00208897	
			0.00208727	

TABLE 2. L_2 norm of computed $\frac{\partial L}{\partial \rho}$ for number of stored corrections $m = 1, 3, 5$ on adaptively refined meshes for example 1.

To get data at the observation points we solve the elastic wave equation with 4 pulses, initialized as described above, with the exact value of the parameters $\rho = 9$ and Lamé coefficients $\lambda = 1.2, \mu = 1.0$ inside the domain, forming a pyramid (see Fig. 1), and $\rho = 1, \lambda = 0.7, \mu = 0.5$ in the rest of the domain.

We start the optimization algorithm with $\rho = 1.0, \lambda = 0.7, \mu = 0.5$ at the points of the computational domain. We choose $T = 2.4$. The computations were performed on three times adaptively refined meshes. The numbers of the nodes and elements in these meshes are presented in the Table 8. The relative time T_{rel} in the table is computed as

$$(8.3) \quad T_{rel} = \frac{t}{S \cdot n},$$

where t is the total time, S is number of the time steps, n is number of the nodes in computational mesh. The experiments were performed with numbers of the timesteps $S = 500$.

After each optimization iteration we perform a smoothing procedure. The values of the parameters are smoothed by local averaging over neighboring elements.

In Tables 2, 4, 3 we present computed L_2 norms of $\frac{\partial L}{\partial \rho}, \frac{\partial L}{\partial \lambda}, \frac{\partial L}{\partial \mu}$ on different adaptively refined meshes. Computed L_2 norms of $v - v_{obs}$ are presented in Table 5. The computed results are presented in the tables as long as the L_2 norm of $v - v_{obs}$ decreases. For example, as follows from Table 5, we perform 5 optimization iterations for a one times refined mesh, consisting of 5426 nodes. Note, that computed gradients are not always decreasing.

m	2783 nodes	5426 nodes	7062 nodes	10951
1	0.000149256	0.000133998	0.0001397	0.000143417
	0.000135338	0.000130628	0.000131215	0.000118576
	2.94165e-06	4.27581e-06	2.05726e-05	8.05369e-05
	3.45666e-06	3.99716e-06	7.59000e-06	5.99590e-05
		3.44076e-06		4.57060e-05
		5.10362e-06		4.46198e-05
3	0.000149256	0.000133998	0.000139700	0.000143417
	0.000143729	2.11378e-05	0.000142738	4.55883e-05
	7.22935e-06	3.99766e-06	1.02584e-05	6.67478e-05
	3.82620e-06	3.87200e-06		2.92434e-05
	3.64912e-06	3.40289e-06		
5	0.000149256	0.000133998	0.000139700	0.000143417
	0.000143729	0.000134093	0.000142738	4.55883e-05
	7.22935e-06	2.11378e-05	1.02584e-05	2.92434e-05
	3.88045e-06	7.83398e-05	2.22772e-05	
	3.75613e-06	3.99766e-06	1.81725e-05	
	3.14287e-06			

TABLE 3. L_2 norm of computed $\frac{\partial L}{\partial \mu}$ for number of stored corrections $m = 1, 3, 5$ on adaptively refined meshes for example 1

m	2783 nodes	5426 nodes	7062 nodes	10951
1	4.43669e-05	4.23986e-05	4.7745e-05	5.26378e-05
	4.28028e-05	4.19256e-05	4.66106e-05	5.57142e-05
	1.14407e-06	1.61033e-06	8.42204e-06	3.74848e-05
	2.02356e-06	1.53588e-06	3.71544e-06	2.75300e-05
	1.42240e-06	1.33757e-06		2.17506e-05
3	4.43669e-05	4.23986e-05	4.77450e-05	5.26378e-05
	4.41308e-05	4.27280e-05	4.9111e-05	5.49515e-05
	2.82406e-06	9.51082e-06	5.8852e-06	2.11851e-05
	1.40884e-06	1.48928e-06		3.08300e-05
		1.47970e-06		
5	4.43669e-05	4.23986e-05	4.77450e-05	5.26378e-05
	4.41308e-05	4.27280e-05	4.9111e-05	5.49515e-05
	2.82406e-06	9.51082e-06	5.8852e-06	2.11851e-05
	1.43332e-06	1.48928e-06	1.19441e-05	
	1.38929e-06	1.45147e-06	1.02565e-05	
	1.25239e-06			

TABLE 4. L_2 norm of computed $\frac{\partial L}{\partial \lambda}$ for number of stored corrections $m = 1, 3, 5$ on adaptively refined meshes for example 1.

m	2783 nodes	5426 nodes	7062 nodes	10951
1	0.0477582	0.0446024	0.0440170	0.0451579
	0.0462955	0.0435771	0.0420571	0.0434939
	0.0145835	0.0162211	0.0150877	0.0151879
	0.0137544	0.0158132	0.0148014	0.0128771
3		0.0139463		
	0.0477582	0.0446024	0.0440170	0.0451579
	0.0473327	0.0443000	0.0438192	0.0450454
	0.0206492	0.0236196	0.0142122	0.0153117
5		0.0168969		0.0143382
		0.0142188		
	0.0477582	0.0446024	0.0440170	0.0451579
	0.0473327	0.0443000	0.0438192	0.0450454
	0.0206492	0.0236196	0.0142122	0.0153117
	0.0163788	0.0132180	0.0141148	
	0.0162989		0.013564	
	0.0157247			

TABLE 5. L_2 norm of computed $v - v_{obs}$ for number of stored corrections $m = 1, 3, 5$ on adaptively refined meshes for example 1.

The computed parameters ρ , λ and μ on adaptively refined meshes are shown in Fig. 5 – 10.

8.2. Example 2. In this example experiments are performed with 6 spherical pulses, initialized in Ω_{FDM} at the points with coordinates $(0.45, 2.2, 1.25)$, $(1.25, 2.2, 1.25)$, $(2.05, 2.2, 1.25)$, $(2.95, 2.2, 1.25)$, $(3.75, 2.2, 1.25)$ and $(4.55, 2.2, 1.25)$, using absorbing boundary conditions on the outer boundary of Ω_{FDM} . In Fig. 2 we present the computed exact solution of the problem (3.1) inside Ω_{FEM} .

We use the same observation points as for Example 1. We present in Table 6 computed L_2 norms of $\frac{\partial L}{\partial \rho}$, $\frac{\partial L}{\partial \mu}$, $\frac{\partial L}{\partial \lambda}$, respectively, on different adaptively refined meshes. Computed L_2 norms of $v - v_{obs}$ are presented in Table 7.

We note that increasing the storage beyond 5 corrections will not have a very big effect: the time, required to compute the Hessian will increase with no increase in accuracy.

Note that the construction of the grid after each refinement procedure is a quite difficult task: we should keep two layers of the structured nodes unchanged at the overlapping boundaries with Ω_{FDM} , which are involved in the exchange procedure. Only the nodes from Ω_{FEM} are involved in the adaptive refinement algorithm keeping the structured Ω_{FDM} grid unchanged.

8.3. Example 3. We performed also experiments with 6 spherical pulses as described in Example 2 and with adding noise to the data at the observation points. We added 10% and 20% noise to the exact solution on the finest mesh at the observation nodes. In Fig. 12 we present the solution at one observation point without and with added noise. In Table 12

L_2 norm	opt.it.	2783 nodes	5426 nodes	7062 nodes	10951
$\frac{\partial L}{\partial \rho}$	1	0.000782747	0.000595812	0.00560402	0.000555752
	2	0.000765166	0.000591426	0.00058001	0.000553765
	3	0.000102281	0.000366747	0.000351486	0.000397794
	4		0.000318678	0.000310022	0.00019666
	5			0.000239935	
$\frac{\partial L}{\partial \mu}$	1	6.29329e-06	5.32755e-06	1.24844e-05	2.12138e-05
	2	6.22415e-06	5.31403e-06	1.24828e-05	1.41816e-05
	3	5.88679e-07	4.27431e-06	8.6882e-06	
	4	2.91749e-06	3.53481e-06	5.34646e-06	
	5	8.9528e-08		5.09221e-06	
$\frac{\partial L}{\partial \lambda}$	1	2.51563e-06	2.05807e-06	6.12897e-06	9.09655e-06
	2	2.48780e-06	2.05127e-06	5.37243e-06	6.24897e-06
	3	3.12468e-07	5.18086e-08	5.26930e-06	
	4	3.44241e-07	4.51412e-08	1.71642e-06	
	5	7.10301e-08			
	6	6.60916e-08			

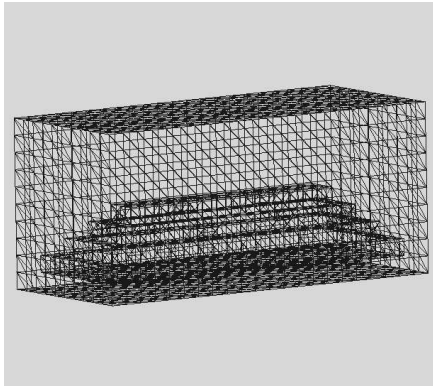
TABLE 6. L_2 norm of computed $\frac{\partial L}{\partial \rho}$, $\frac{\partial L}{\partial \lambda}$, $\frac{\partial L}{\partial \mu}$ for number of stored corrections $m = 3$ on adaptively refined meshes for example 2.

opt.it.	2783 nodes	5426 nodes	7062 nodes	10951
1	0.00972044	0.00876599	0.00847722	0.0085713
2	0.00970074	0.00876608	0.00194653	0.0024212
3	0.00266514	0.00150852	0.00164972	
4	0.00205583	0.00113243	0.00158979	
5	0.00196030			

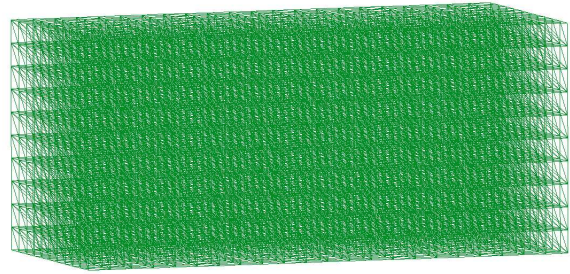
TABLE 7. L_2 norm of computed $v - v_{obs}$ for number of stored corrections $m = 3$ on adaptively refined meshes for example 2.

No. of nodes	No. of elements	Forward problem		Adjoint problem	
		relat.time	time, sec	relat.time	time, sec
2783	13200	5.6001e-05	31.17	1.2192e-04	67.860
5426	27450	5.6395e-05	61.20	1.2816e-04	139.08
7062	36560	5.5593e-05	78.52	1.2983e-04	183.36
10951	57716	5.6520e-05	123.79	1.2921e-04	283.1

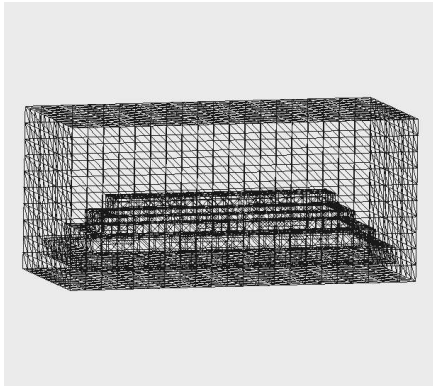
TABLE 8. Performance in the relative time (at the left column) and in the total time (at the right column) for the Forward and the Adjoint problems for Example 2.



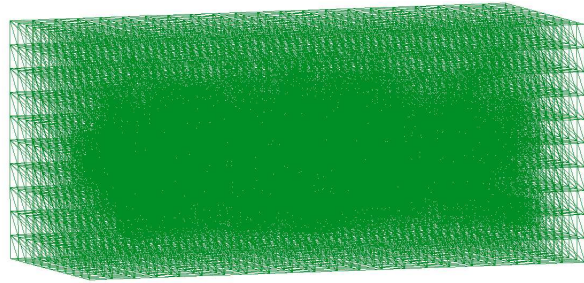
a) coarse mesh



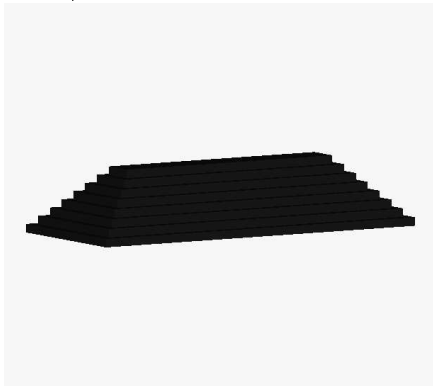
b) coarse mesh



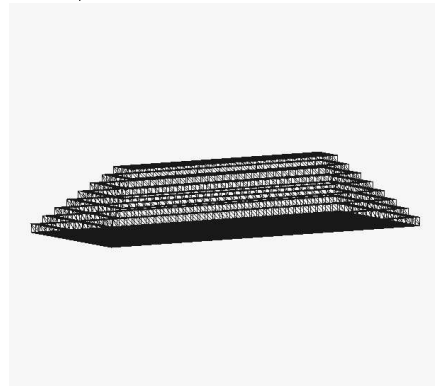
c) 3 times refined mesh



d) 3 times refined mesh



e) exact object



f) exact object, mesh

FIGURE 1. Computational FEM meshes. In a), c) we present only boundary nodes for different types of materials and in b), d) we show all nodes in the meshes.

L_2 norm	opt.it.	2783 nodes	5426 nodes	7062 nodes	10951
$\frac{\partial L}{\partial \rho}$	1	0.000793030	0.000604759	0.00568072	0.000563051
	2	0.000784028	0.000600191	0.00056560	0.000561018
	3	0.000173019	0.000651657	0.000545401	0.000555309
	4	0.000109423	0.000411288	0.000568119	0.000214045
	5	0.000378875	0.000138286	0.000272153	
	6			0.000114470	
	7			0.000197248	
$\frac{\partial L}{\partial \mu}$	1	6.35025e-06	5.36721e-06	1.23378e-05	2.10536e-05
	2	6.28055e-06	5.35406e-06	1.23384e-05	2.11365e-05
	3	1.50998e-06	5.59563e-06	9.14679e-06	2.14829e-05
	4	8.16513e-07	4.27406e-06	9.81399e-06	1.5932e-05
	5		1.44231e-06		9.29962e-06
$\frac{\partial L}{\partial \lambda}$	1	2.53522e-06	2.07213e-06	6.16055e-06	9.06972e-06
	2	2.50746e-06	2.06548e-06	6.17416e-06	9.10238e-06
	3	7.40625e-07	2.17085e-06	5.57219e-06	9.23918e-06
	4	2.80418e-07	1.62479e-06	5.80515e-06	6.65874e-06
	5	1.42559e-06	4.79122e-07	1.08050e-05	3.93673e-06
	6			4.87839e-06	2.77268e-06

TABLE 9. L_2 norm of computed $\frac{\partial L}{\partial \rho}$, $\frac{\partial L}{\partial \lambda}$, $\frac{\partial L}{\partial \mu}$ for number of stored corrections $m = 5$ on adaptively refined meshes. We add 10% noise to the data at the observation points.

we present computed L_2 norms of $v - v_{obs}$ on different adaptively refined meshes. As we see from the results, it is possible reconstruct the object with 10% noise. We get a more nonsmooth solution with 20% noise at the observation points, but a reconstruction is still possible. The reconstructed parameters λ and μ with added 10% noise to the data at the observation points are shown in Fig.11.

8.4. Example 4. We now present numerical tests for the reconstruction of a single cube. We perform similar tests as in the previous examples, but with $T = 2.6$ and 300 time steps.

We start the optimization algorithm with $\rho = 1.0, \lambda = \mu = 0.5$ at all points of the computational domain. The computations was performed on five times adaptively refined meshes. In Table 13 we shown computed L_2 norms of $v - v_{obs}$ on different adaptively refined meshes, presented in Fig. 13. The computational tests show, that the best results are obtained on a 4 times adaptively refined mesh. The values of the identified parameters are very sensitive to the starting values of the parameters in the optimization algorithm and to the type of regularization of the solution. In this example we have chosen different start values for these parameters: $\gamma_\rho = 1.0, \gamma_\mu = 1.0, \gamma_\lambda = 0.1$. We present the reconstructed parameters ρ, λ and μ on a 4 times adaptively refined mesh – in Fig. 14.

opt.it.	2783 nodes	5426 nodes	7062 nodes	10951
1	0.0098186	0.00888107	0.00859326	0.00870716
2	0.00979883	0.00888174	0.00859704	0.00871430
3	0.00456252	0.00888583	0.00898915	0.00875216
4	0.00360370	0.00870797	0.00914326	0.00494146
5		0.00457173	0.00659696	0.00159288
6		0.00168708	0.00381484	

TABLE 10. L_2 norm of computed $v - v_{obs}$ for number of stored corrections $m = 3$ on the adaptively refined meshes. We add 10% noise to the data at the observation points.

L_2 norm	opt.it.	2783 nodes	5426 nodes	7062 nodes	10951
$\frac{\partial L}{\partial \rho}$	1	0.000803408	0.000613880	0.000575969	0.000570631
	2	0.000794023	0.000609121	0.000573435	0.000568556
	3	0.000636853	0.000640811	0.000569044	0.000568038
	4	0.000776814	0.000645965	0.000569602	
$\frac{\partial L}{\partial \mu}$	1	6.40861e-06	5.40844e-06	1.22147e-05	2.0931e-05
	2	6.33835e-06	5.39568e-06	1.2218e-05	2.10118e-05
	3	5.05217e-06	5.53357e-06	9.30845e-06	2.12367e-05
	4	6.46414e-06	4.93732e-06		
	5	1.02650e-07	3.8590e-06		
$\frac{\partial L}{\partial \lambda}$	1	2.55542e-06	2.0869e-06	6.20131e-06	9.05891e-06
	2	2.50009e-06	2.0804e-06	6.21642e-06	9.091e-06
	3	2.33451e-06	2.14802e-06	5.44857e-06	9.19938e-06
	4	2.80418e-07	1.91414e-06		
	5	1.42559e-06	1.4077e-06		

TABLE 11. L_2 norm of computed $\frac{\partial L}{\partial \rho}$, $\frac{\partial L}{\partial \lambda}$, $\frac{\partial L}{\partial \mu}$ for number of stored corrections $m = 3$ on adaptively refined meshes. We add 20% noise to the data at the observation points.

opt.it.	2783 nodes	5426 nodes	7062 nodes	10951
1	0.00992072	0.00900206	0.00871874	0.00884980
2	0.00990097	0.00900321	0.0087228	0.008885724
3	0.00917995	0.00901267	0.00885476	0.0089102
4		0.00310553	0.00215861	0.00279184
5			0.00212623	0.00278610

TABLE 12. L_2 norm of computed $v - v_{obs}$ for number of stored corrections $m = 3$ on adaptively refined meshes. We add 20% noise to the data at the observation points.

opt.it.	2783 nodes	2847 nodes	3183 nodes	3771 nodes	4283 nodes	6613 nodes
1	0.00522332	0.00514721	0.00512072	0.0049972	0.00498482	0.00471736
2	0.00508603	0.00501885	0.00500625	0.00489408	0.00488648	0.00462337
3	0.00453599	0.00455756		0.00410481	0.00431073	0.00433048
4	0.00438557	0.00417061		0.00362429	0.0034339	0.00415263
5		0.00384466		0.00327727	0.00331261	
6					0.00233499	
7					0.00213977	

TABLE 13. Reconstruction of a cube. L_2 norm of computed $v - v_{obs}$ for number of stored corrections $m = 5$ on five times adaptively refined meshes.

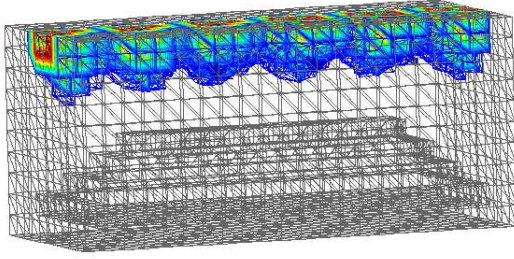
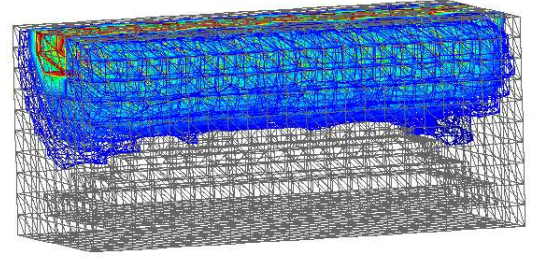
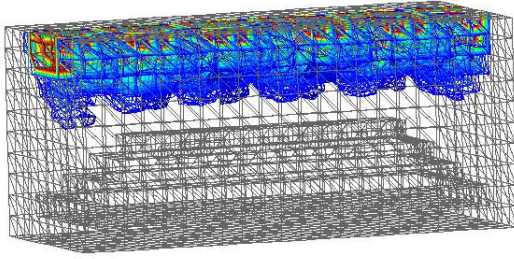
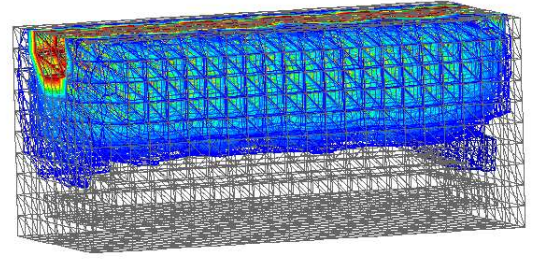
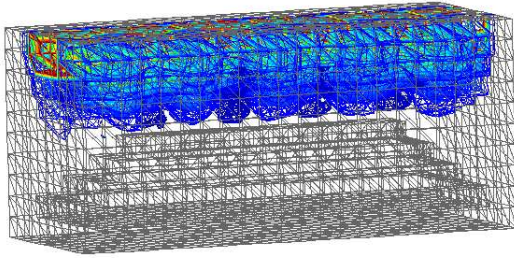
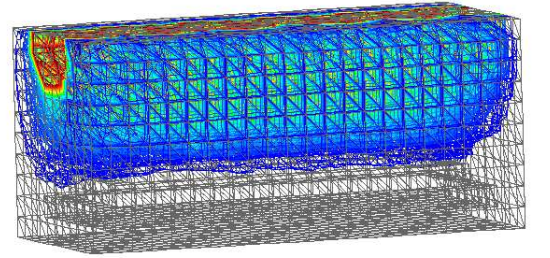
 $t = 0.4$  $t = 1.2$  $t = 0.6$  $t = 1.6$  $t = 0.8$  $t = 1.8$

FIGURE 2. The exact solution in Ω_{FEM} with mesh size $h = 0.2$. On the boundary Ω_{FDM} we apply absorbing boundary conditions. The exact value of the parameters are $\rho = 25, \mu = 1.0, \lambda = 1.0$ inside domain, forming a cone (see Fig. 1), and $\rho = 1, \mu = 0.5, \lambda = 0.5$ at the rest of the domain. We present also the location of different isosurfaces.

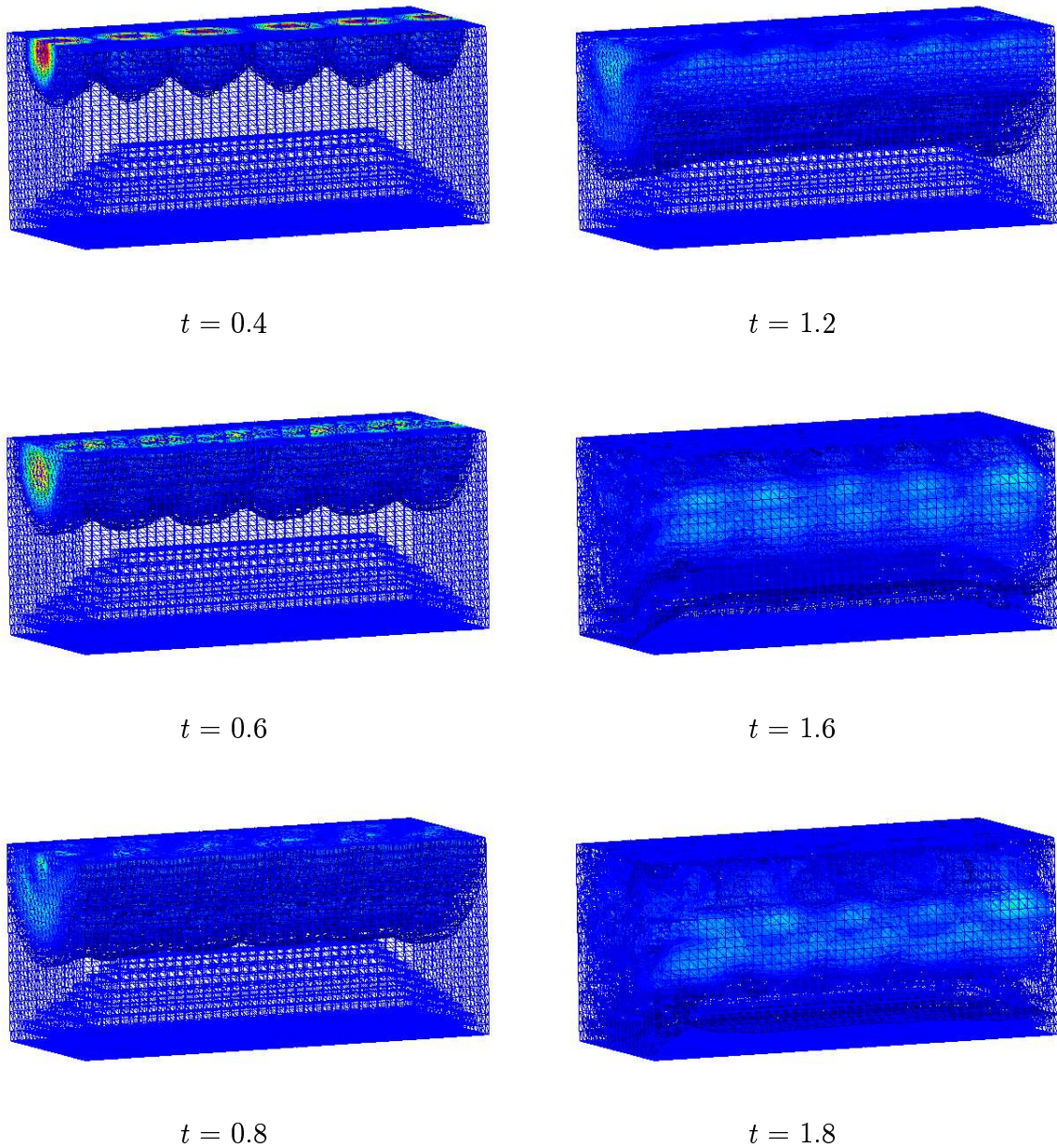


FIGURE 3. The exact solution in Ω_{FEM} with mesh size $h = 0.1$. On the boundary Ω_{FDM} we apply absorbing boundary conditions. The exact value of the parameters are $\rho = 9, \mu = 1.0, \lambda = 1.2$ inside domain, forming a pyramid (see Fig. 1), and $\rho = 1, \mu = 0.5, \lambda = 0.7$ at the rest of the domain. We present also the location of different isosurfaces.

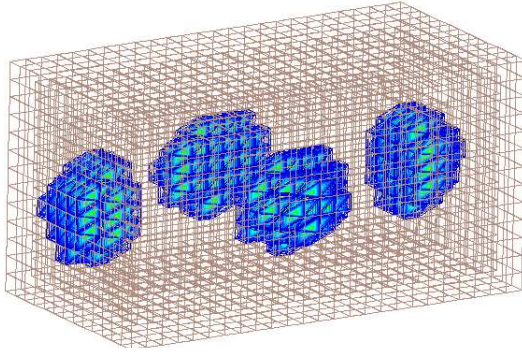
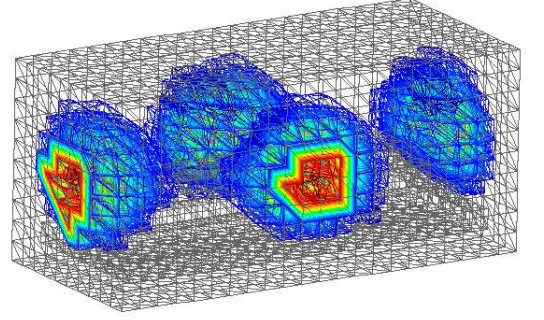
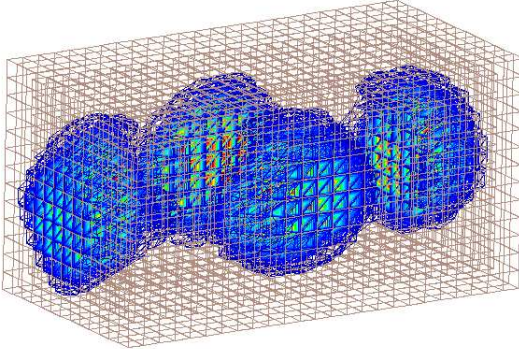
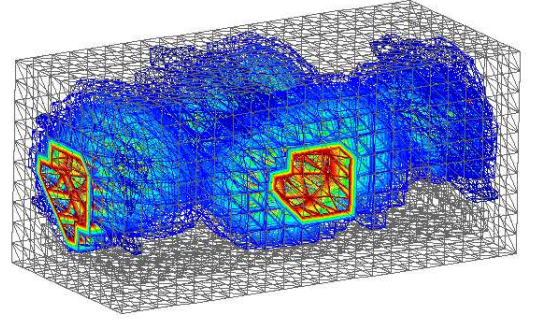
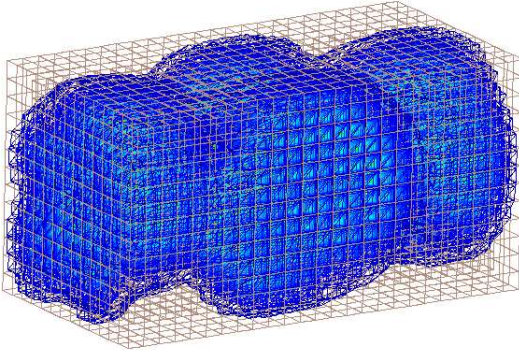
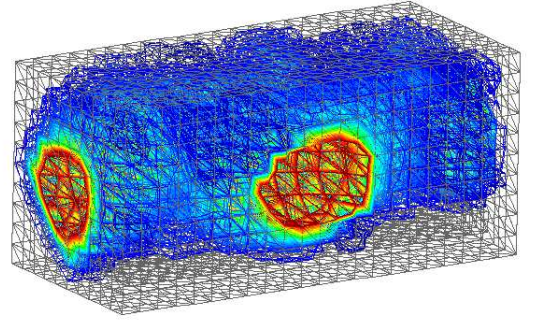
a) $t = 0.2$ d) $t = 0.2$ b) $t = 0.4$ e) $t = 0.4$ c) $t = 0.7$ f) $t = 0.7$

FIGURE 4. The exact solution for Example 2. On the boundary Ω_{FDM} we apply absorbing boundary conditions. The exact value of the parameters are $\rho = 9.0, \mu = 1.0, \lambda = 1.2$ inside domain, forming a cone (see Fig. 1), and $\rho = 1, \mu = 0.5, \lambda = 0.7$ at the rest of the domain. In a), b), c) we present the location of the different isosurfaces in Ω_{FDM} and in d), e) , f) the corresponding solutions are presented in Ω_{FEM} .

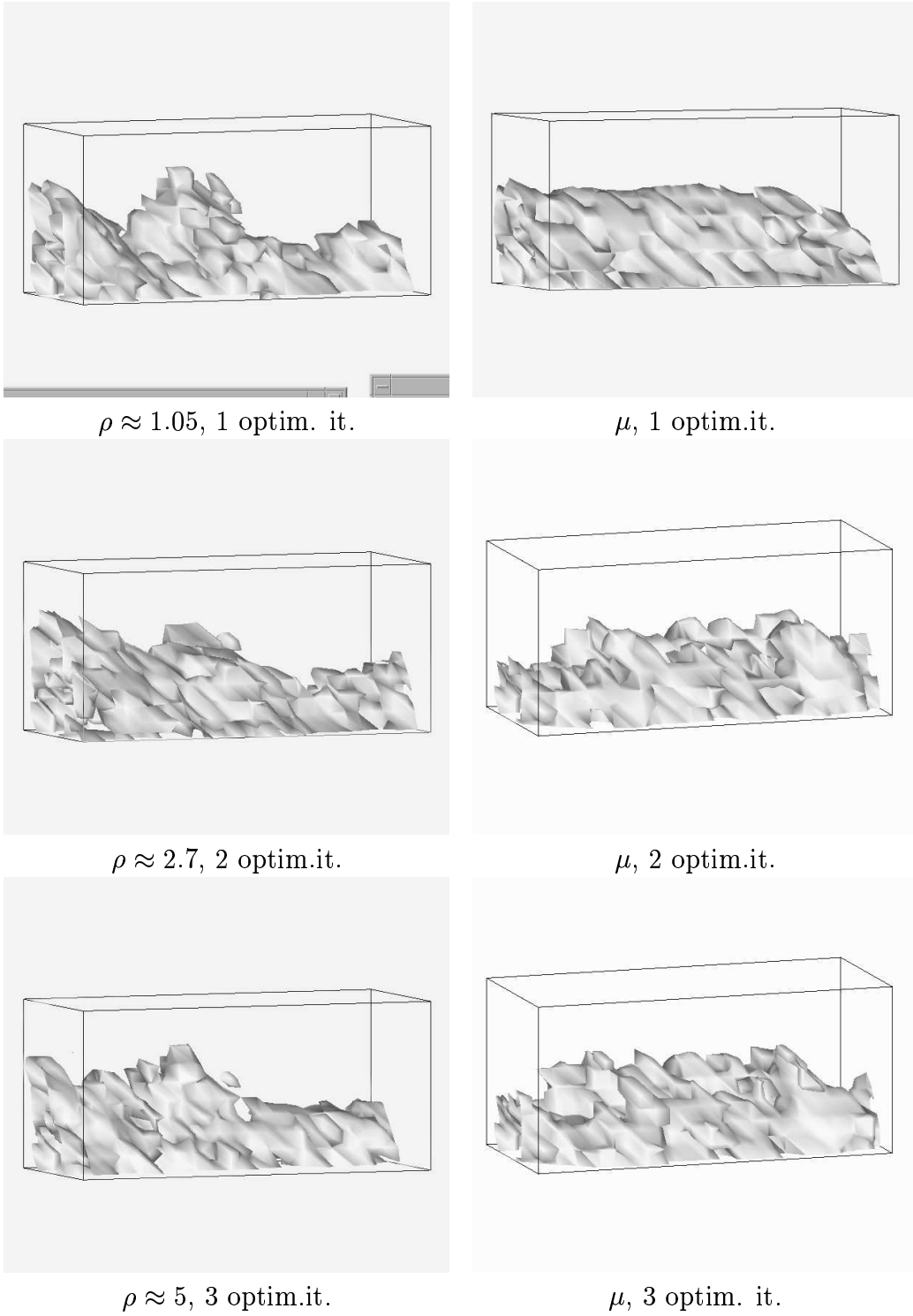
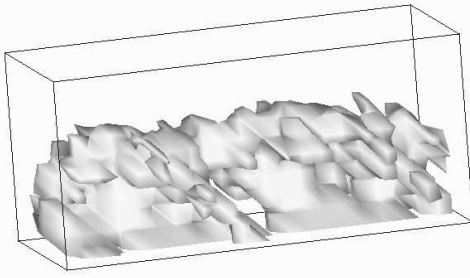
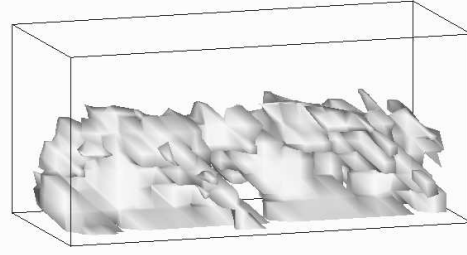


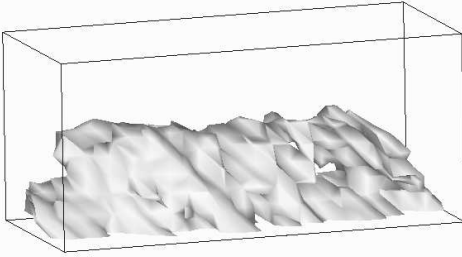
FIGURE 5. Reconstructed parameters ρ and μ on the coarse mesh after first, second and third optimization iterations. The value of the isosurface for ρ is shown on the reconstruction picture, while the value of the isosurface for $\mu \approx 0.56$.



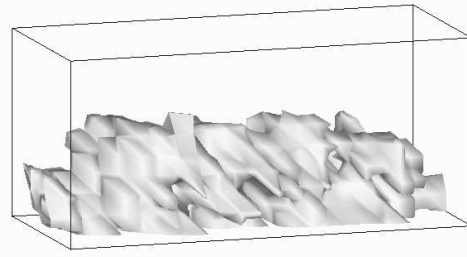
λ , after 1 optim. it., $m=1$



λ , after 1 it., $m=3$



λ , after 2 optim.it., $m=1$



λ , after 3 optim.it., $m=1$

FIGURE 6. Reconstructed parameter λ on the coarse mesh after first, second and third optimization iterations. The value of the isosurface is ≈ 0.6 .

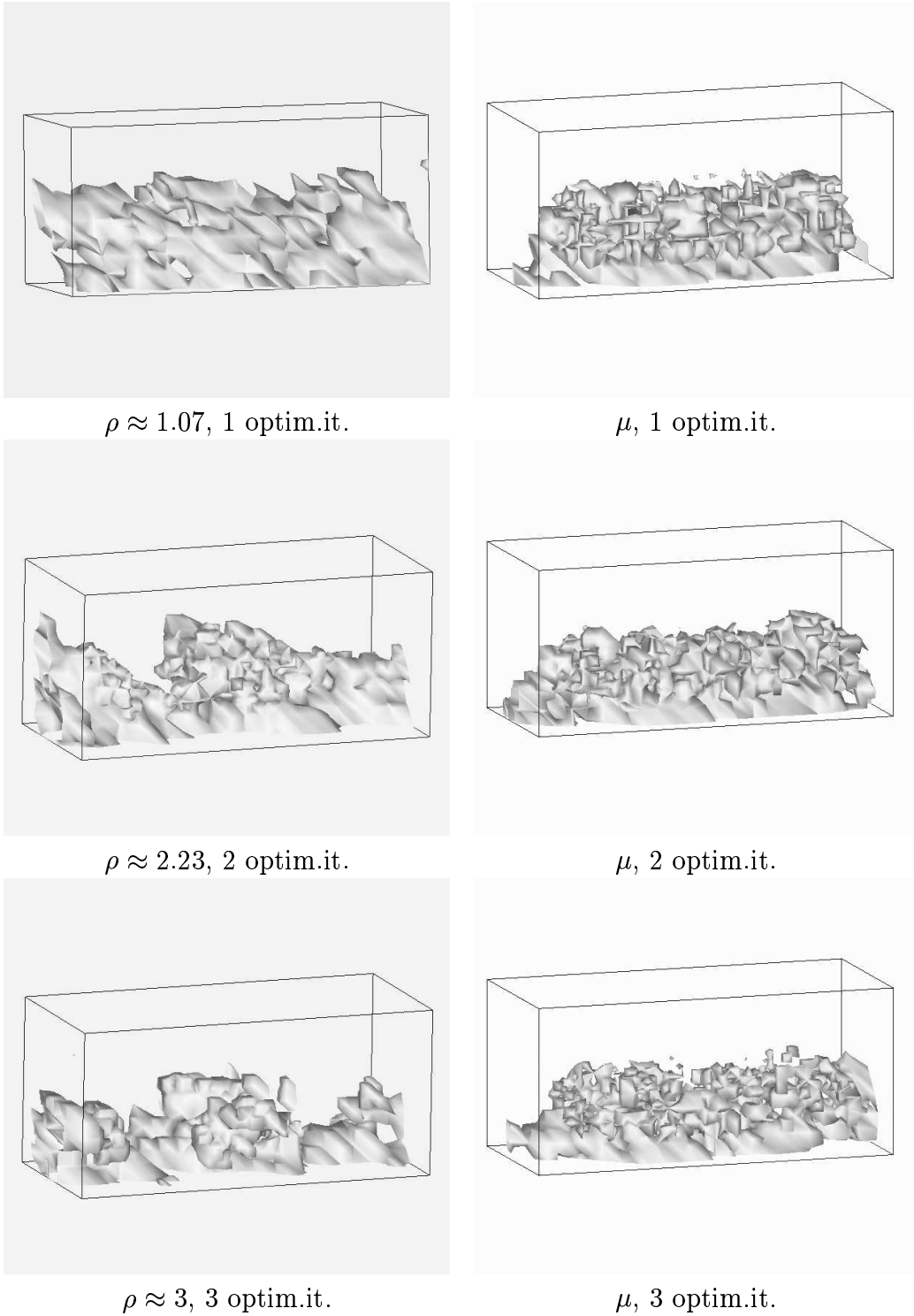


FIGURE 7. Reconstructed parameters ρ and μ on the one time adaptively refined mesh after first, second and third optimization iterations. The value of the isosurface for density is ≈ 25 , while the value of the isosurface for $\mu \approx 0.8$.

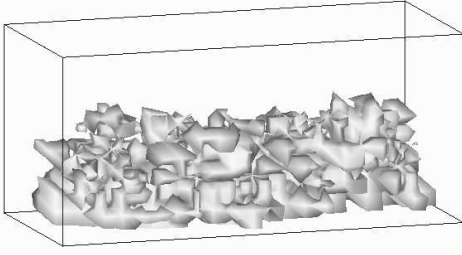
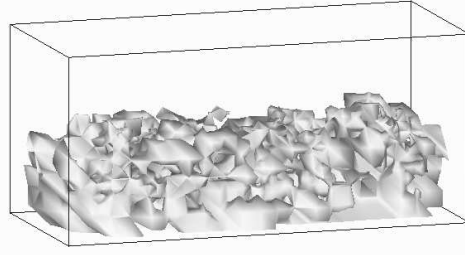
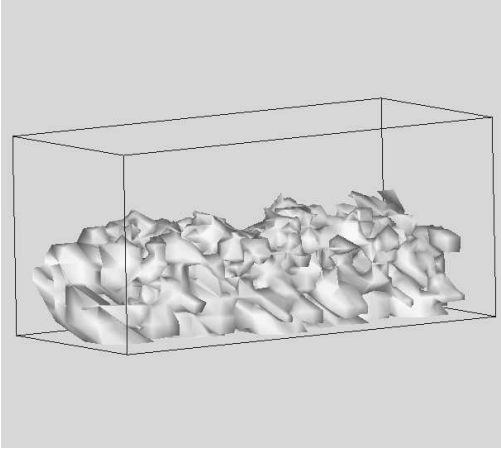
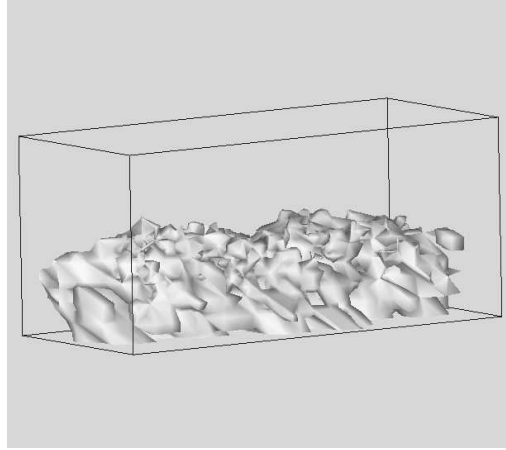
 λ , after 1 optim.it. λ , after 2 optim.it. λ , after 3 optim. it. λ , after 4 optim.it.

FIGURE 8. Reconstructed parameter λ on the one time adaptively refined mesh after first, second and third optimization iterations. The value of the isosurface is ≈ 0.8 .

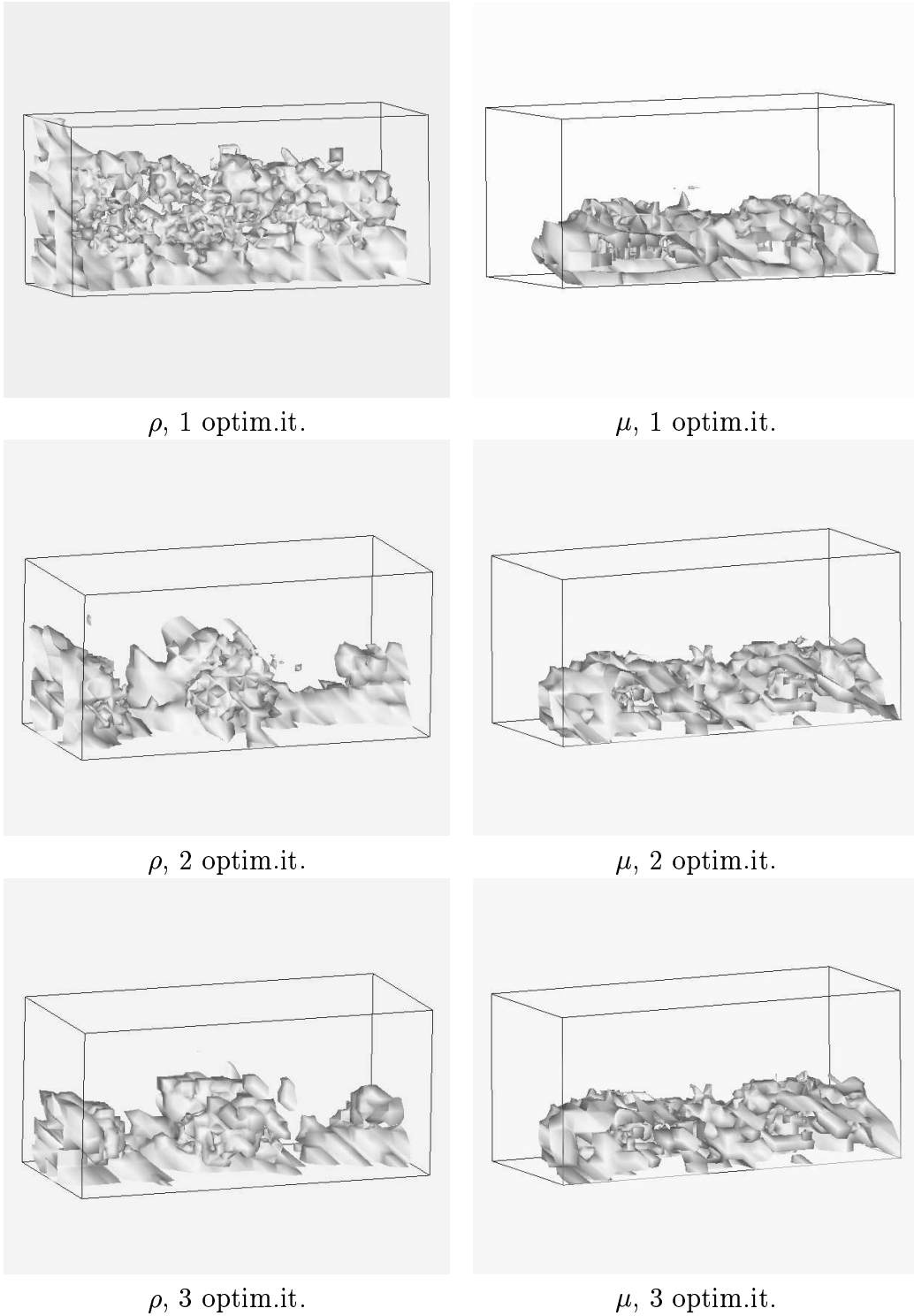


FIGURE 9. Reconstructed parameters ρ and μ for Example 3 on the two times adaptively refined mesh after first, second and third optimization iterations. The value of the isosurface for density is ≈ 2 , while the value of the isosurface for $\mu \approx 0.6$.

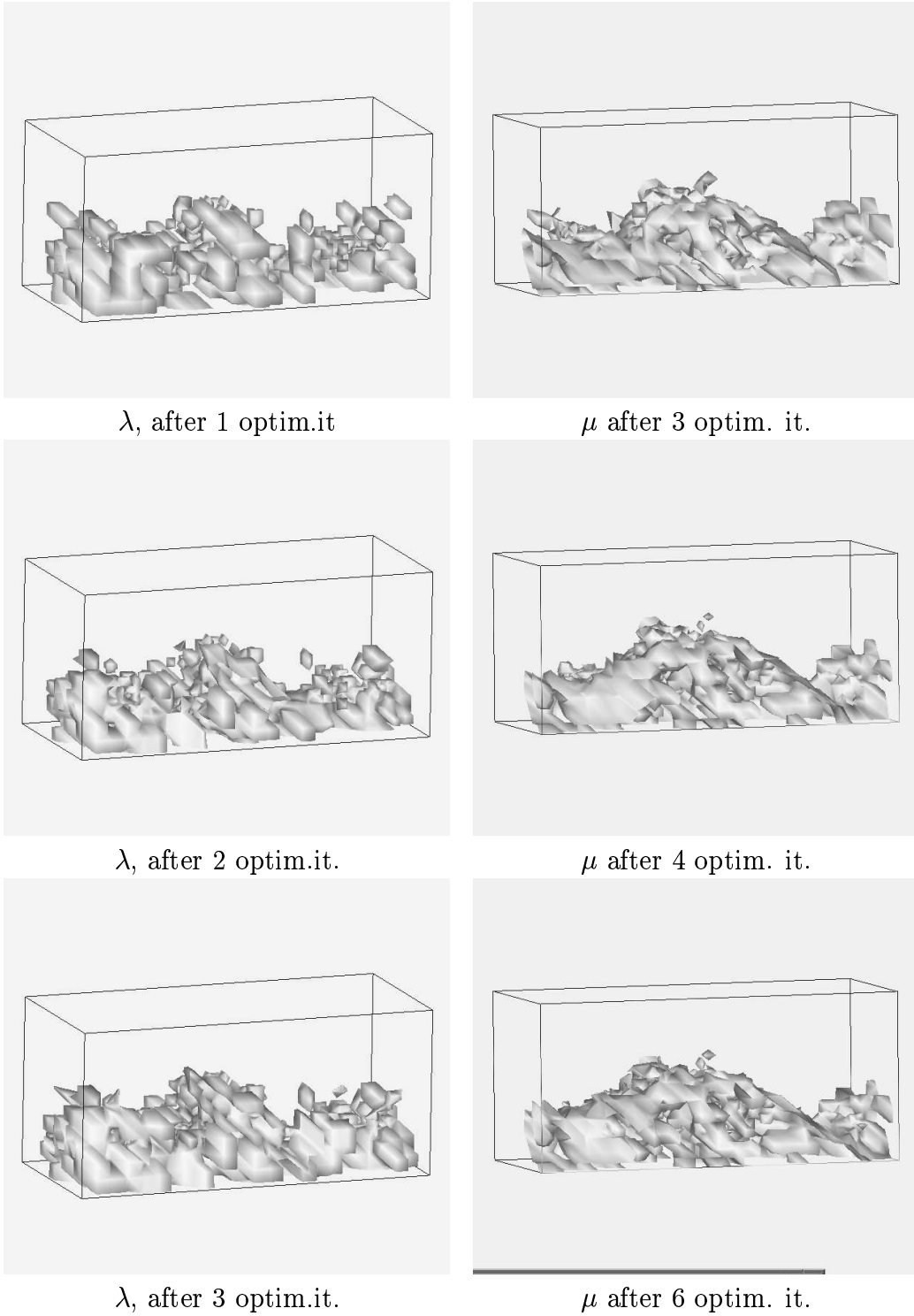
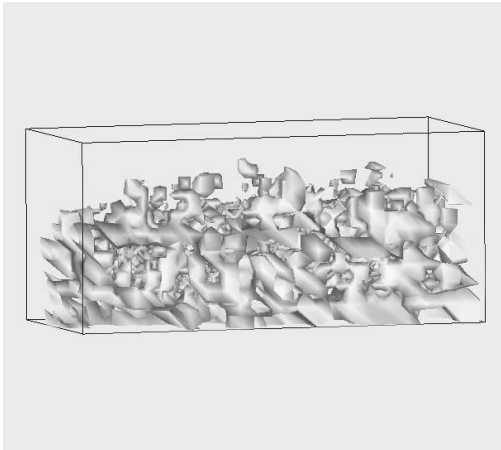
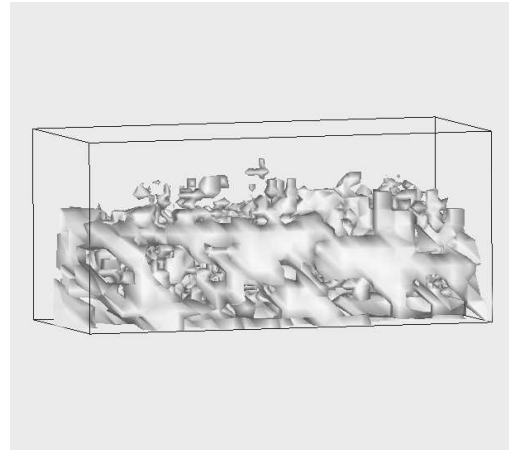


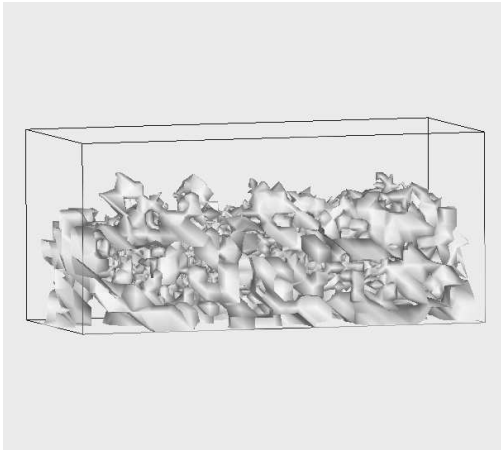
FIGURE 10. Reconstructed parameter λ for Example 3 on the two times adaptively refined mesh after first, second and third optimization iterations. The values of the isosurfaces are ≈ 0.74 .



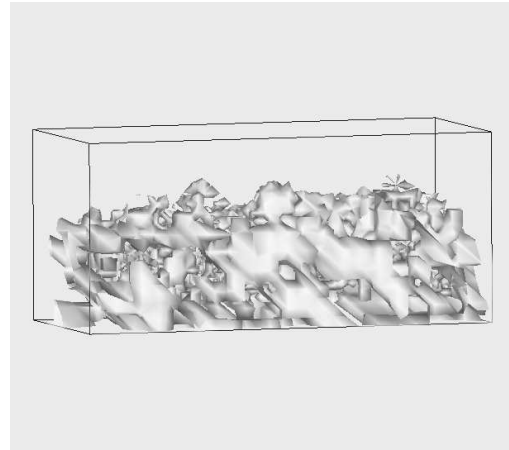
$\lambda \approx 0.75$, after 3 optim.it



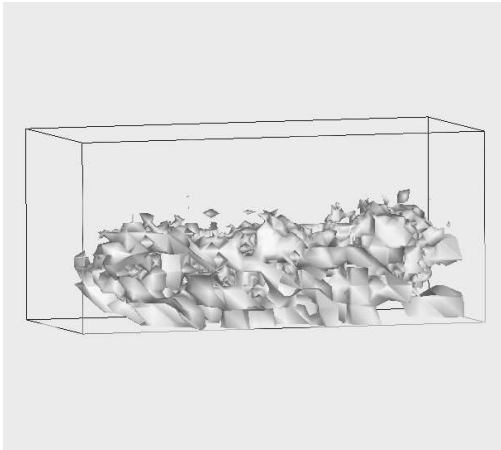
$\mu \approx 0.55$ after 3 optim. it.



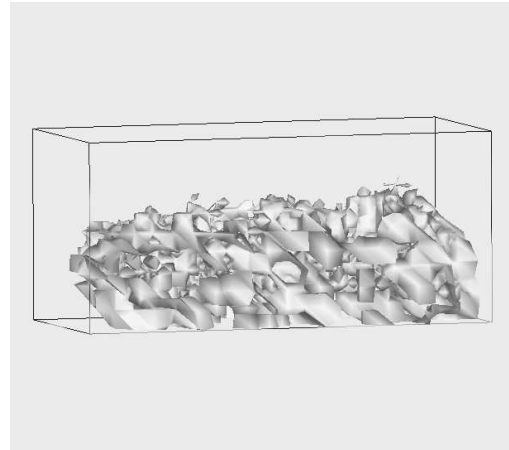
$\lambda \approx 0.85$, after 4 optim.it.



$\mu \approx 0.65$ after 4 optim. it.



$\lambda \approx 1.0$, after 5 optim.it.



$\mu \approx 0.87$ after 7 optim. it.

FIGURE 11. Reconstructed parameters λ and μ on the 3 times adaptively refined mesh with adding 10% noise to the exact data.

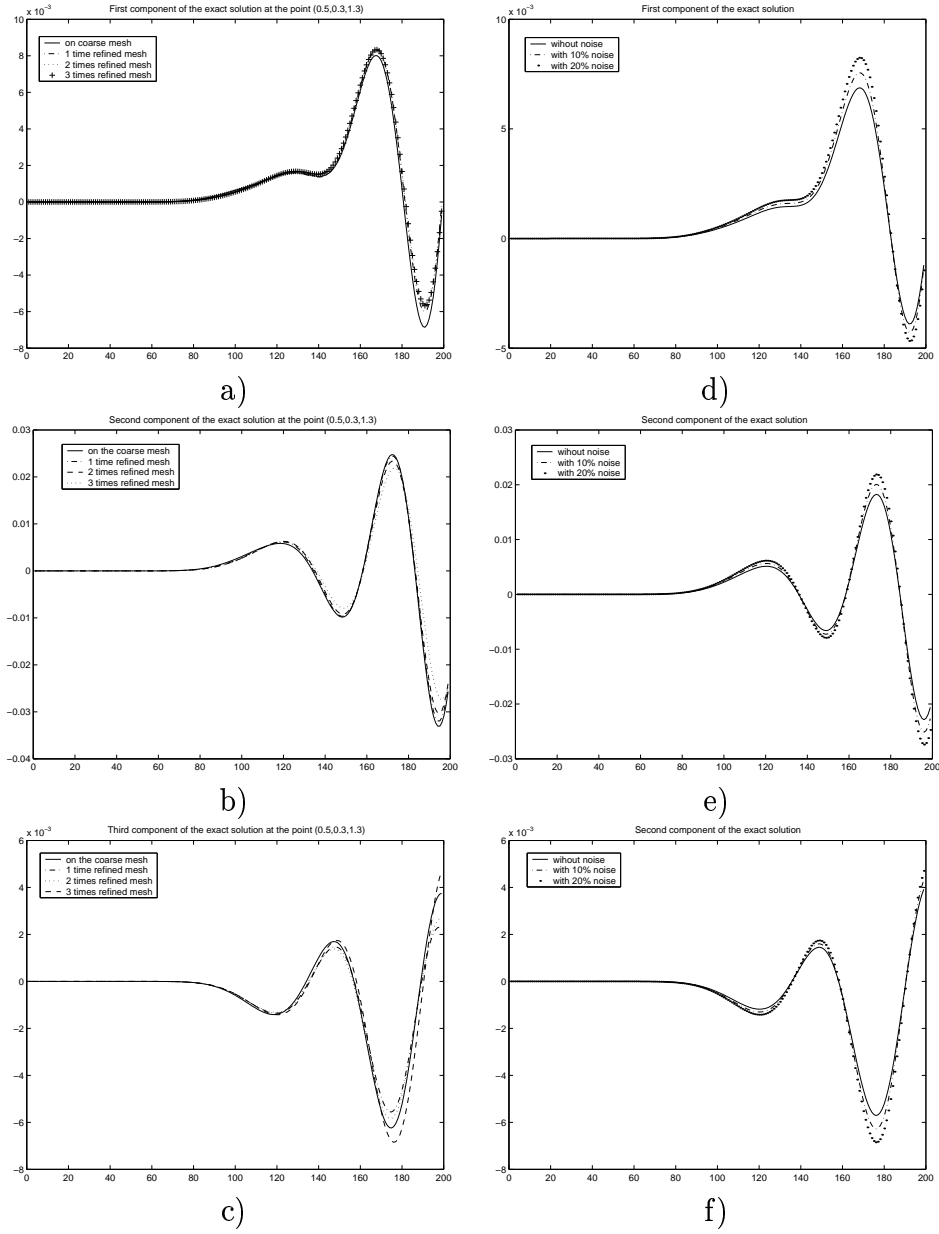
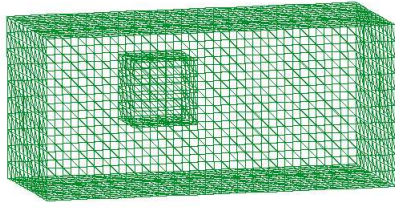
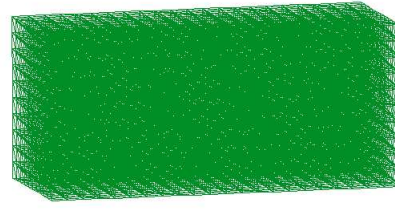


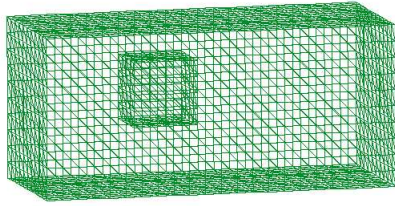
FIGURE 12. Exact solution at the one point $(0.5, 0.3, 1.3)$. We show three components of the solution on the different adaptively refined meshes in a), b), c), In d), e) f) we show the solution at the one point on the three times adaptively refined mesh without noise and with adding noise.



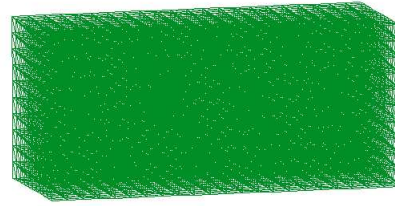
a) 2783 nodes, boundary nodes



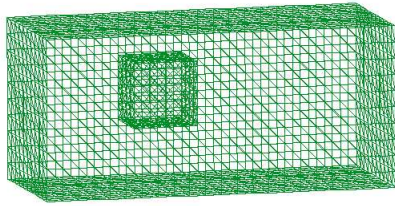
d) 2783 nodes, all nodes



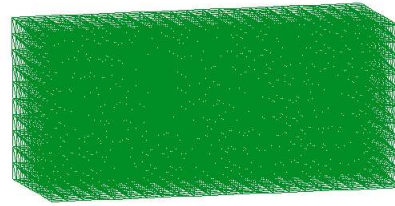
b) 2847 nodes, boundary nodes



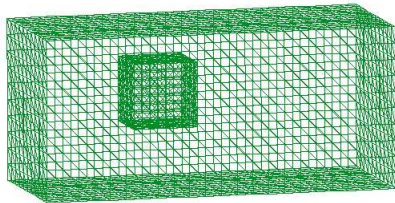
e) 2847 nodes, all nodes



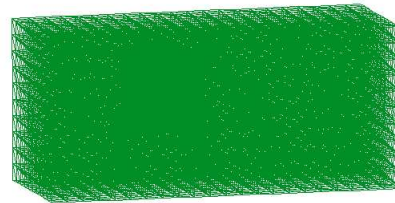
c) 3183 nodes, boundary nodes



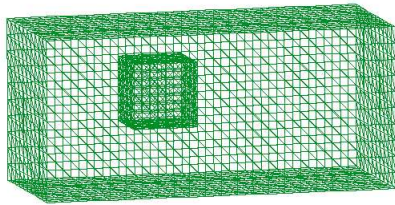
f) 3183 nodes, all nodes



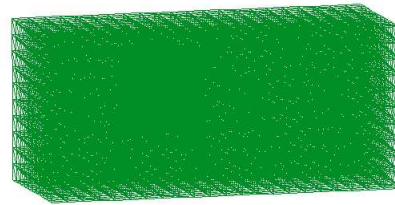
c) 3771 nodes, boundary nodes



f) 3771 nodes, all nodes



c) 4283 nodes, boundary nodes



f) 4283 nodes, all nodes

FIGURE 13. Adaptively refined grids for reconstruction of a cube.

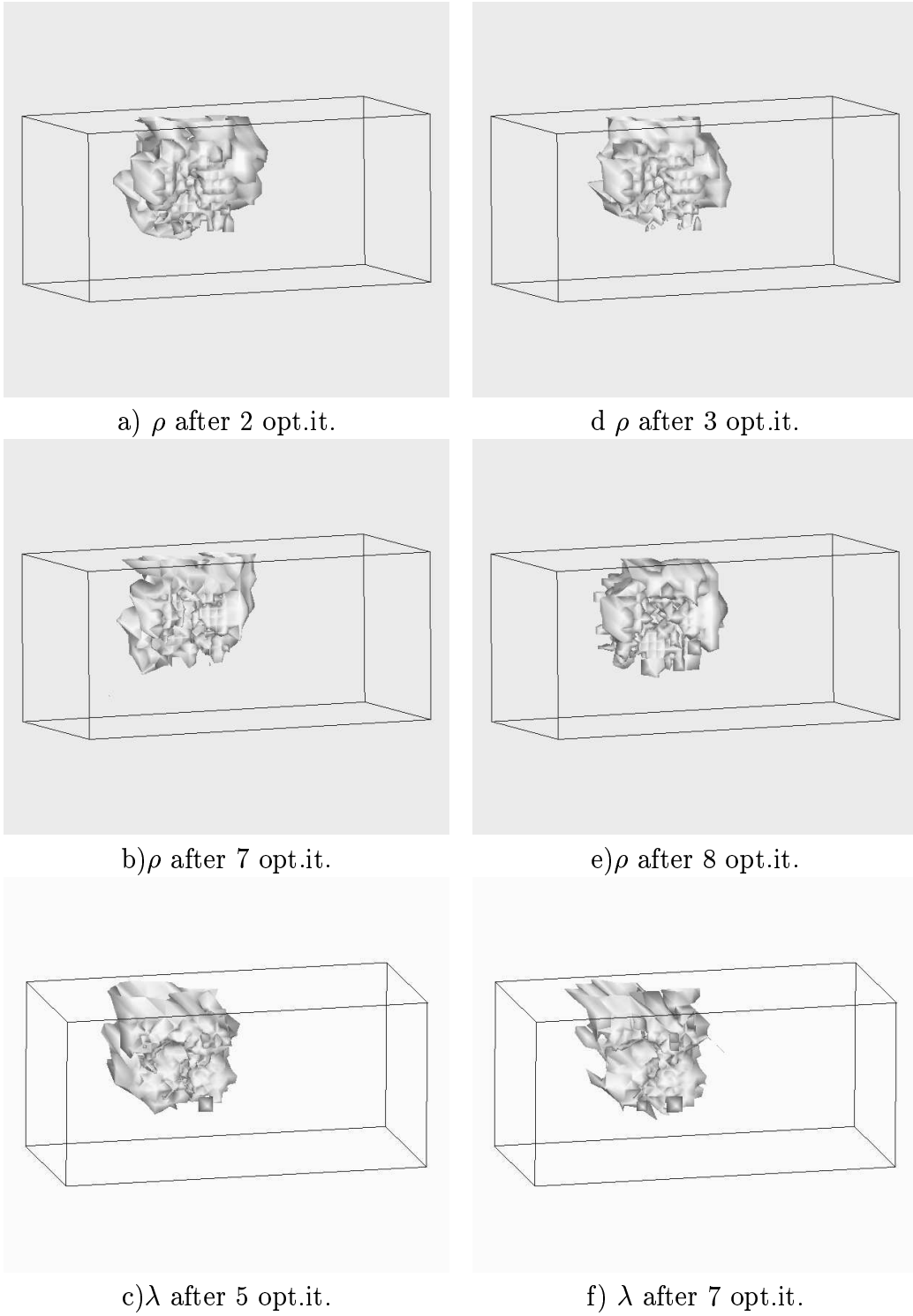


FIGURE 14. Reconstruction of a cube. We show reconstructed parameters ρ and λ on four times adaptively refined mesh.

REFERENCES

- [1] B. Auld, Acoustic fields and waves in solids Vol.2, ISBN 990090687X, Malabar, Krieger, 1990.
- [2] E. Acklam, A. Jacobsen and H.P. Langtangen, Optimizing C++ code for explicit finite difference schemes, Oslo Scientific Computing Archive, Report 1998-4.
- [3] S. Balay, W. Gropp, L-C. McInnes, B. Smith, PETSc user manual, <http://www.mcs.anl.gov/petsc>
- [4] R. Becker, Adaptive finite elements for optimal control problems, Habilitationsschrift, Heidelberg, 2001.
- [5] J. Cea, A numerical method for the computation of an optimal domain. Lecture notes in computer sciences, Vol. 41, Springer, New York, 1976.
- [6] C. Douglas, J. Hu, M. Kowarschik, U. R  de and C. Weiss, Cache optimization for structured and unstructured grid multigrid, ETNA volume 10, pp.21-40, 2000.
- [7] V. Barbu, Analysis and control of nonlinear infinite dimensional systems, Mathematics in Science and Engineering, Volume 190, 1993.
- [8] L. Beilina, K. Samuelsson, K.   hl  nder, A hybrid method for the wave equation. Proceedings of International Conference on Finite Element Methods, Gakuto International Series Mathematical Sciences and Applications, Gakkotosho CO., LTD, 2001.
- [9] L. Beilina, Adaptive finite element method for an inverse scattering problem, J. Inverse Problems and Information Technologies, Vol.1, 2003, to appear.
- [10] L. Beilina, A hybrid method for elastic waves, J. Applied and Computational Mathematics, Vol.2, to appear.
- [11] G. C. Cohen, Higher Order numerical methods for transient wave equations, Springer Verlag Berlin Heidelberg New York, 2002.
- [12] F. Edelvik, U. Andersson, and G. Ledfelt, Hybrid finite volume - finite difference solver for the Maxwell equations, In AP2000 Millennium Conference on Antennas & Propagation, Davos, Switzerland, 2000.
- [13] F. Edelvik and G. Ledfelt, Explicit hybrid time domain solver for the Maxwell equations in 3D, J. Sci. Comput., 2000.
- [14] B. Engquist, A. Majda, Absorbing boundary conditions for the numerical simulation of waves, Math. Comp., Volume 31, number 139, p.629-651, 1977.
- [15] K. Eriksson, D. Estep and C. Johnson, Computational Differential Equations, Studentlitteratur, Lund, 1996.
- [16] R. Fletcher, Practical methods of optimization, John Wiley and Sons, Ltd, 1986.
- [17] P.C. Hansen, Rank-deficient and discrete ill-posed problems, SIAM, Philadelphia, 1998.
- [18] T. J. R. Hughes, The Finite Element Method. Prentice Hall, 1987.
- [19] S. C. Brenner, L. R. Scott, The Mathematical theory of finite element methods, Springer-Verlag, 1994.
- [20] F. Ihlenburg, Finite Element Analysis of Acoustic Scattering. ISBN 0-387-98319-8, Springer-Verlag New York Berlin Heidelberg, 1998.
- [21] J.L. Lions, Optimal control of systems governed by partial differential equations, Springer-Verlag, New York, 1971.
- [22] F. Murat and J. Simon, Studies on optimal shape design problems, Lecture Notes in Computer Science 41, Springer-Verlag, Berlin 1976.
- [23] F. Natterer, F. Wubbeling, Mathematical Methods in Image reconstruction, SIAM, 2001.
- [24] F. Natterer, An initial value approach to the inverse Helmholtz problem at fixed frequency, Proceeding of the Conference in Oberwolfach, Springer, 1997.
- [25] F. Natterer, A finite difference method for the inverse scattering problem at fixed frequency (with F. Wubbeling), Proceedings of the Lapland conference on Inverse Problems, 1992.

- [26] J. Nečas, I. Hlavaček, Mathematical theory of elastic and elasto-plastic bodies: an introduction, Studies in applied mechanics 3, Elsevier scientific publishing company, Amsterdam-Oxford-New York, 1981.
- [27] P. Neittaanmäki, D. Tiba, Optimal Control of nonlinear parabolic systems, Pure and applied mathematics, Marcel Dekker, USA, 1994.
- [28] J. Haslinger, P. Neittaanmäki, Finite Element Approximation for optimal shape design: theory and applications, John Wiley & Sons LTD, 1988.
- [29] J. Nocedal, Updating quasi-Newton matrices with limited storage, J. Mathematical of Comp., V. 35, N. 151, pp.773-782.
- [30] O. Pironneau, Optimal shape design for elliptic systems, Springer Verlag, 1984.
- [31] E. Polak, Computational methods in optimization, Academic, New York, 1971.

Chalmers Finite Element Center Preprints

- 2001–01 *A simple nonconforming bilinear element for the elasticity problem*
Peter Hansbo and Mats G. Larson
- 2001–02 *The \mathcal{LL}^* finite element method and multigrid for the magnetostatic problem*
Rickard Bergström, Mats G. Larson, and Klas Samuelsson
- 2001–03 *The Fokker-Planck operator as an asymptotic limit in anisotropic media*
Mohammad Asadzadeh
- 2001–04 *A posteriori error estimation of functionals in elliptic problems: experiments*
Mats G. Larson and A. Jonas Niklasson
- 2001–05 *A note on energy conservation for Hamiltonian systems using continuous time finite elements*
Peter Hansbo
- 2001–06 *Stationary level set method for modelling sharp interfaces in groundwater flow*
Nahidh Sharif and Nils-Erik Wiberg
- 2001–07 *Integration methods for the calculation of the magnetostatic field due to coils*
Marzia Fontana
- 2001–08 *Adaptive finite element computation of 3D magnetostatic problems in potential formulation*
Marzia Fontana
- 2001–09 *Multi-adaptive galerkin methods for ODEs I: theory & algorithms*
Anders Logg
- 2001–10 *Multi-adaptive galerkin methods for ODEs II: applications*
Anders Logg
- 2001–11 *Energy norm a posteriori error estimation for discontinuous Galerkin methods*
Roland Becker, Peter Hansbo, and Mats G. Larson
- 2001–12 *Analysis of a family of discontinuous Galerkin methods for elliptic problems: the one dimensional case*
Mats G. Larson and A. Jonas Niklasson
- 2001–13 *Analysis of a nonsymmetric discontinuous Galerkin method for elliptic problems: stability and energy error estimates*
Mats G. Larson and A. Jonas Niklasson
- 2001–14 *A hybrid method for the wave equation*
Larisa Beilina, Klas Samuelsson and Krister Åhlander
- 2001–15 *A finite element method for domain decomposition with non-matching grids*
Roland Becker, Peter Hansbo and Rolf Stenberg
- 2001–16 *Application of stable FEM-FDTD hybrid to scattering problems*
Thomas Rylander and Anders Bondeson
- 2001–17 *Eddy current computations using adaptive grids and edge elements*
Y. Q. Liu, A. Bondeson, R. Bergström, C. Johnson, M. G. Larson, and K. Samuelsson
- 2001–18 *Adaptive finite element methods for incompressible fluid flow*
Johan Hoffman and Claes Johnson
- 2001–19 *Dynamic subgrid modeling for time dependent convection-diffusion-reaction equations with fractal solutions*
Johan Hoffman

- 2001–20** *Topics in adaptive computational methods for differential equations*
Claes Johnson, Johan Hoffman and Anders Logg
- 2001–21** *An unfitted finite element method for elliptic interface problems*
Anita Hansbo and Peter Hansbo
- 2001–22** *A P^2 -continuous, P^1 -discontinuous finite element method for the Mindlin-Reissner plate model*
Peter Hansbo and Mats G. Larson
- 2002–01** *Approximation of time derivatives for parabolic equations in Banach space: constant time steps*
Yubin Yan
- 2002–02** *Approximation of time derivatives for parabolic equations in Banach space: variable time steps*
Yubin Yan
- 2002–03** *Stability of explicit-implicit hybrid time-stepping schemes for Maxwell's equations*
Thomas Rylander and Anders Bondeson
- 2002–04** *A computational study of transition to turbulence in shear flow*
Johan Hoffman and Claes Johnson
- 2002–05** *Adaptive hybrid FEM/FDM methods for inverse scattering problems*
Larisa Beilina
- 2002–06** *DOLFIN - Dynamic Object oriented Library for FINite element computation*
Johan Hoffman and Anders Logg
- 2002–07** *Explicit time-stepping for stiff ODEs*
Kenneth Eriksson, Claes Johnson and Anders Logg
- 2002–08** *Adaptive finite element methods for turbulent flow*
Johan Hoffman
- 2002–09** *Adaptive multiscale computational modeling of complex incompressible fluid flow*
Johan Hoffman and Claes Johnson
- 2002–10** *Least-squares finite element methods with applications in electromagnetics*
Rickard Bergström
- 2002–11** *Discontinuous/continuous least-squares finite element methods for elliptic problems*
Rickard Bergström and Mats G. Larson
- 2002–12** *Discontinuous least-squares finite element methods for the Div-Curl problem*
Rickard Bergström and Mats G. Larson
- 2002–13** *Object oriented implementation of a general finite element code*
Rickard Bergström
- 2002–14** *On adaptive strategies and error control in fracture mechanics*
Per Heintz and Klas Samuelsson
- 2002–15** *A unified stabilized method for Stokes' and Darcy's equations*
Erik Burman and Peter Hansbo
- 2002–16** *A finite element method on composite grids based on Nitsche's method*
Anita Hansbo, Peter Hansbo and Mats G. Larson
- 2002–17** *Edge stabilization for Galerkin approximations of convection-diffusion problems*
Erik Burman and Peter Hansbo

- 2002-18** *Adaptive strategies and error control for computing material forces in fracture mechanics*
Per Heintz, Fredrik Larsson, Peter Hansbo and Kenneth Runesson
- 2002-19** *A variable diffusion method for mesh smoothing*
J. Hermansson and P. Hansbo
- 2003-01** *A hybrid method for elastic waves*
L.Beilina
- 2003-02** *Application of the local nonobtuse tetrahedral refinement techniques near Fichera-like corners*
L.Beilina, S.Korotov and M. Krížek
- 2003-03** *Nitsche's method for coupling non-matching meshes in fluid-structure vibration problems*
Peter Hansbo and Joakim Hermansson
- 2003-04** *Crouzeix–Raviart and Raviart–Thomas elements for acoustic fluid–structure interaction*
Joakim Hermansson
- 2003-05** *Smoothing properties and approximation of time derivatives in multistep backward difference methods for linear parabolic equations*
Yubin Yan
- 2003-06** *Postprocessing the finite element method for semilinear parabolic problems*
Yubin Yan
- 2003-07** *The finite element method for a linear stochastic parabolic partial differential equation driven by additive noise*
Yubin Yan
- 2003-08** *A finite element method for a nonlinear stochastic parabolic equation*
Yubin Yan
- 2003-09** *A finite element method for the simulation of strong and weak discontinuities in elasticity*
Anita Hansbo and Peter Hansbo
- 2003-10** *Generalized Green's functions and the effective domain of influence*
Donald Estep, Michael Holst, and Mats G. Larson
- 2003-11** *Adaptive finite element/difference method for inverse elastic scattering waves*
L.Beilina

These preprints can be obtained from

www.phi.chalmers.se/preprints